Nucleon Elastic Form Factors
Experiments and Data

Donal Day
University of Virginia

October 28, 2004

Outline

- ✳ Introduction, Motivation and Formalism
- ✳ Traditional Techniques and Data
- ✳ Models
- ✳ Recent Experiments
  - Recoil Polarization
  - Beam-Target Asymmetry
  - Ratio method
  - Rosenbluth & the Discrepancy
- ✳ Prospects and Conclusion

Other Talks at Baryons 04

S. Baunack	Single Spin Asymmetries from the Mainz A4 Experiment
W. Brooks	A precise determination of the neutron magnetic form factor to higher Q^2
B. Desplanques	Dirac's inspired point form and hadron form factors
M. Giannini	Electromagnetic form factors in the hypercentral constituent quark model
M. Gorschtein	Partonic calculation for beam normal spin asymmetry in elastic lepton-nucleon scattering
D. Hasell	Recent results from BLAST
A. Hoell	Covariant Description of nucleon form factors
J. Martin	The strange form factors of the proton and the G_0 collaboration
S. Pacetti	What can we learn about the ratio GEp/GMp
K. Paschke	Second generation HAPPEx experiments
G. Quemener	Experimental review of electroweak form factors
M. Seimetz	Measurement of the electric form factor of the neutron at MAMI
S.Serednyakov	The project of the experimental study of nucleon electromagnetic form factors with VEPP-2000 e^+e^- collider
I. Sick	Nucleon form factors at low momentum transfer
A. Silva	Baryon form factors in the chiral quark-soliton model
E. Tomasi	Two-photon exchange and electromagnetic proton form factors
T. Van Cauteren	Electromagnetic transitions of hyperons in a relativistic quark model
M. Vanderhaeghen	QED radiative corrections to precise measurements of proton elastic form factors

Nucleons have Structure!

Early Indications

- ✳ Anomalous magnetic moments of p and n
  O. Stern, Nature 132 (1933) 169
- ✳ Non-zero neutron charge radius from scattering of thermal neutrons on atoms
- ✳ Experiments on Nucleon Structure go back to the mid 1950's at Stanford, see *Nuclear and Nucleon Structure, R. Hofstader, W.A. Benjamin (1963).*

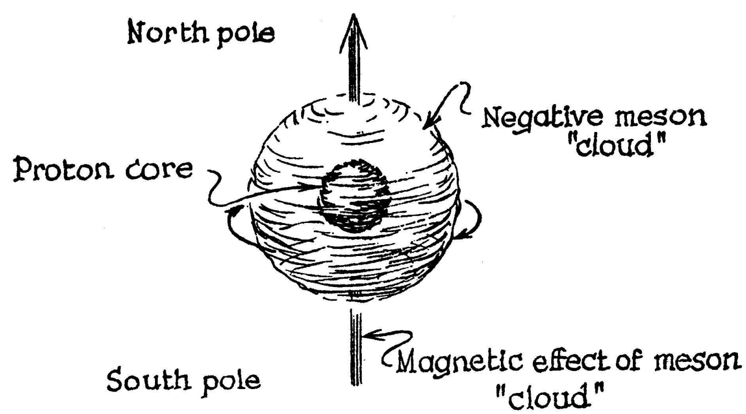

Motivation

- FF are fundamental quantities
- Describe the internal structure of the nucleon
- Provide rigorous tests of QCD description of the nucleon

  Symmetric quark model, with all valence quarks with same wf: $G_E^n \equiv 0$

  $G_E^n \neq 0 \rightarrow$ details of the wavefunctions
- Necessary for study of nuclear structure

  Few body structure functions

50 years of effort has produced much but $\cdots$ what is new?

- New techniques, unexpected behavior, and a reinvigorated theoretical effort have made the last decade one of dynamic progress.

On FF

The few body system is our best source of information about NN potential, FSI and MEC.

Quark spin-dependent interaction breaks the mass degeneracy of the ground state baryons also leads to a segregation of charge within the nucleon. If the perturbing force is more repulsive for quarks with parallel than antiparallel spins, the induced charge radius $< r^2 >_n$ will be negative.

Explains $\langle \mathbf{r}^{\mathbf{2}}_{\mathrm{ch}} \rangle$ of ^{48}Ca as compared to ^{40}Ca

Formalism

$$\frac{d\sigma}{d\Omega} = \sigma_{\mathrm{Mott}} \frac{E'}{E_0} \left\{ (F_1)^2 + \tau \left[2\,(F_1 + F_2)^2 \tan^2(\theta_e) + (F_2)^2 \right] \right\} ; \; F_{1,2} = F_{1,2}(Q^2)$$

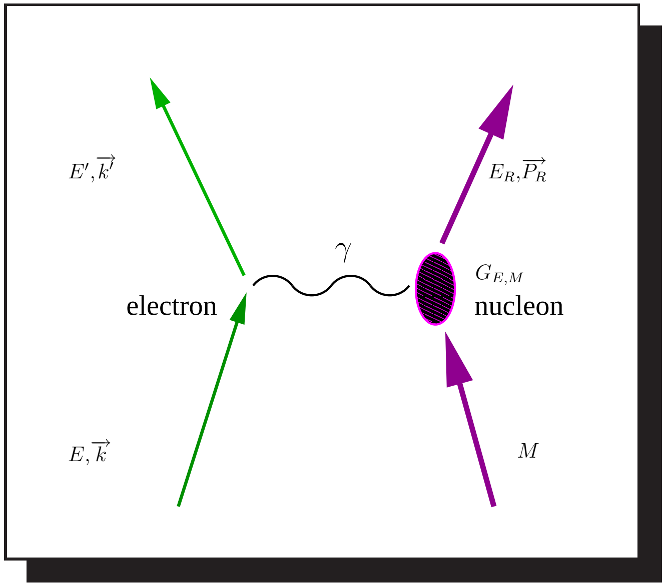

$Q^2 = 4EE' \sin^2(\theta/2)$	$\tau = \frac{Q^2}{4M^2}$
$F_1^p(0) = 1$	$F_1^n(0) = 0$
$F_2^p(0) = 1.79$	$F_2^n(0) = -1.91$

In Breit frame F_1 and F_2 related to charge and spatial curent densities:

$$\rho = J_0 = 2eM[F_1 - \tau F_2]$$

$$J_i = e\bar{u}\gamma_i u[F_1 + F_2]_{i=1,2,3}$$

$$G_E\,(Q^2) = F_1(Q^2) - \tau F_2\,(Q^2) \qquad G_M\,(Q^2) = F_1\,(Q^2) + F_2\,(Q^2)$$

✓ For a point like probe G_E and G_M are the FT of the charge and magnetizations distributions in the nucleon, with the following normalizations

$Q^2 = 0$ limit: $G_E^p = 1$ $G_E^n = 0$ $G_M^p = 2.79$ $G_M^n = -1.91$

one-photon approx.

Rosenbluth formula, separation

$$\frac{d\sigma}{d\Omega} = \sigma_{\rm NS}\left[\frac{G_E^2+\tau G_M^2}{1+\tau} + 2\tau G_M^2 \tan^2(\theta/2)\right]$$

$$\sigma_R \equiv \frac{d\sigma}{d\Omega}\frac{\epsilon(1+\tau)}{\sigma_{\rm NS}} = \underbrace{\tau G_M^2(Q^2)}_{\text{intercept}} + \epsilon \underbrace{G_E^2(Q^2)}_{\text{slope}}$$

① Intercept and slope give G_M and G_E

② G_M dominates for large τ.

③ Must control kinematics, acceptances and radiative corrections.

④ Data consistent with one-photon exchange

$$\boxed{\tau = \frac{Q^2}{4M^2} \quad \epsilon^{-1} = 1 + 2(1+\tau)\tan(\theta/2)^2}$$

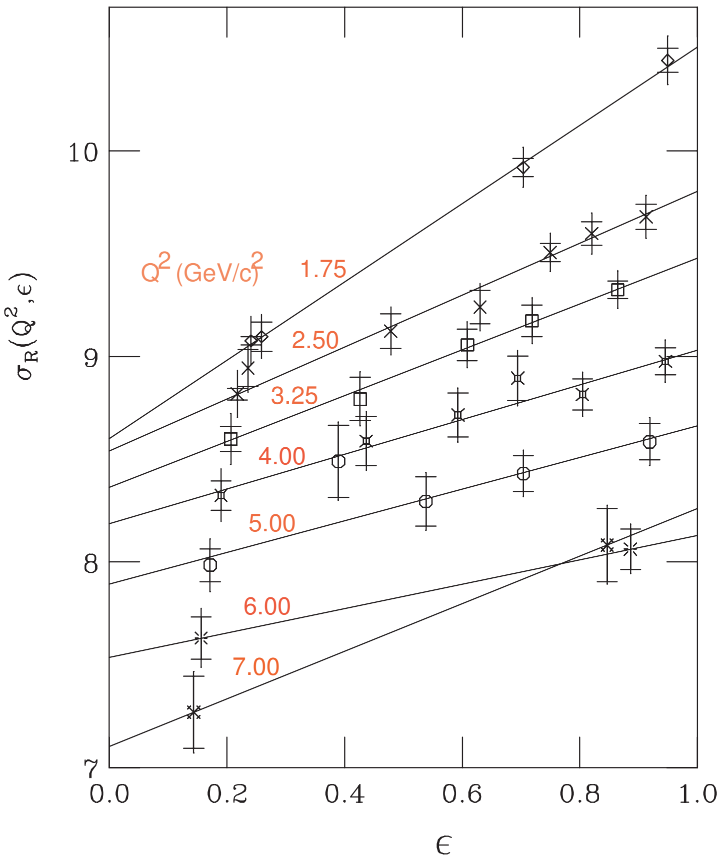

SLAC, Andivahis, Bosted *et al.*

Proton data from Rosenbluth

$$\underbrace{G_E^p(Q^2) \approx \frac{G_M^p(Q^2)}{\mu_p} \approx \frac{G_M^n(Q^2)}{\mu_n}}_{\text{Scaling Law}} \approx \underbrace{G_D \equiv \left(1+\frac{Q^2}{0.71}\right)^{-2}}_{\text{Dipole Law}}$$

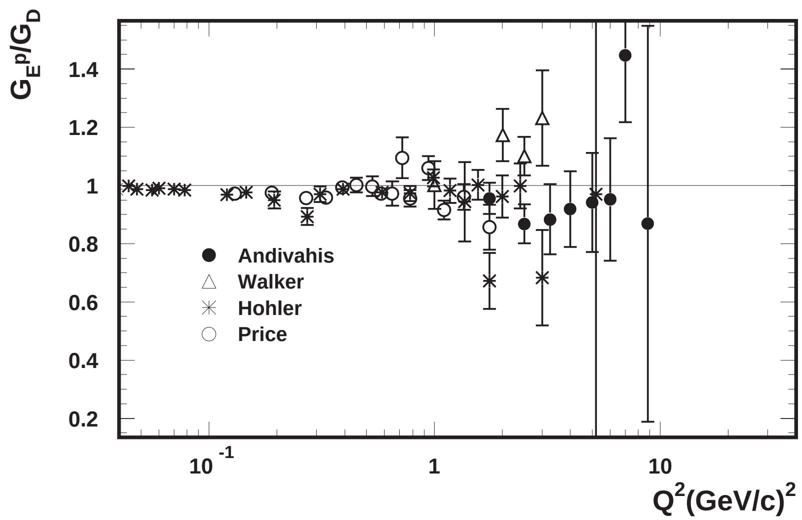

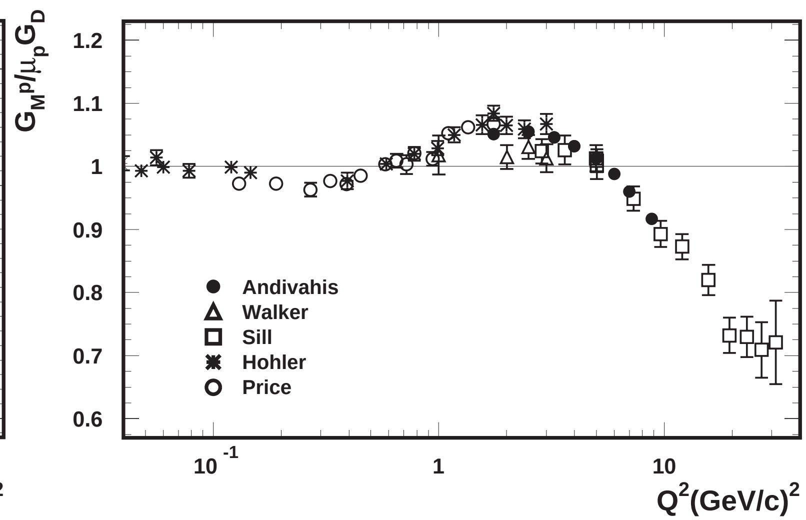

- ✓ G_E^p consistent with G_D, but
  - large uncertainties at large Q^2
  - systematic differences foreshadow limitations of Rosenbluth
- ✓ G_M^p modified relative to G_D at large Q^2

Charge Distribution

Exponential charge distribution, $\rho(r) = \rho_0 e^{-r/r_0}$, generates the dipole form and $G_D = \left(1 + \frac{Q^2}{0.71}\right)$ gives a rms radius of 0.81 fm

Plot of $\sigma_R \equiv \frac{d\sigma}{d\Omega}\frac{\epsilon(1+\tau)}{\sigma_{\mathrm{NS}}}$ taken at fixed Q^2 as a function of ϵ should be a straight line. The intercept of the line is $2\tau G_M^2$, while the slope is G_E^2. Errors in G_E and G_M are determined from the errors in the determination of the slope and intercept.

Linearity of the Rosenbluth formula is based on single photon exchange. As we shall see, this long held assumption is now being reexamined.

Scaling law and dipole scaling are good to 10% up to almost 10 GeV^2.

Traditional techniques to measure Neutron Form Factors

- No neutron target
- proton dominates neutron
- G_M^n dominates G_E^n

G_M^n and G_E^n measured through:

① Elastic scattering ${}^2\mathrm{H}(e,e')^2\mathrm{H}$

② Inclusive quasielastic scattering: ${}^2\mathrm{H}(e,e')X$

③ Exclusive quasielastic: neutron in coincidence: ${}^2\mathrm{H}(e,e'n)p$

④ Ratio techniques $\frac{d(e,e'n)p}{d(e,e'p)n}$ (quasielastic)

Complications: Rosenbluth, subtraction of proton

Even with simplest nucleus – no escaping nuclear physics

No free neutron targets – scattering from a nucleus, D, ^{3}He

Neutron is not free - can not avoid engaging the details of the nuclear physics.

Minimize sensitivity to the how the reaction is treated and maximize the sensitivity to the neutron form factors by working in quasifree kinematics.

CLAS

- Ratio techniques $\frac{d(e,e'n)p}{d(e,e'p)n}$ minimizes roles of g.s. wavefunction and FSI.
- ratio techniques demand careful calibration of neutron detector efficiency.

G_M^n unpolarized

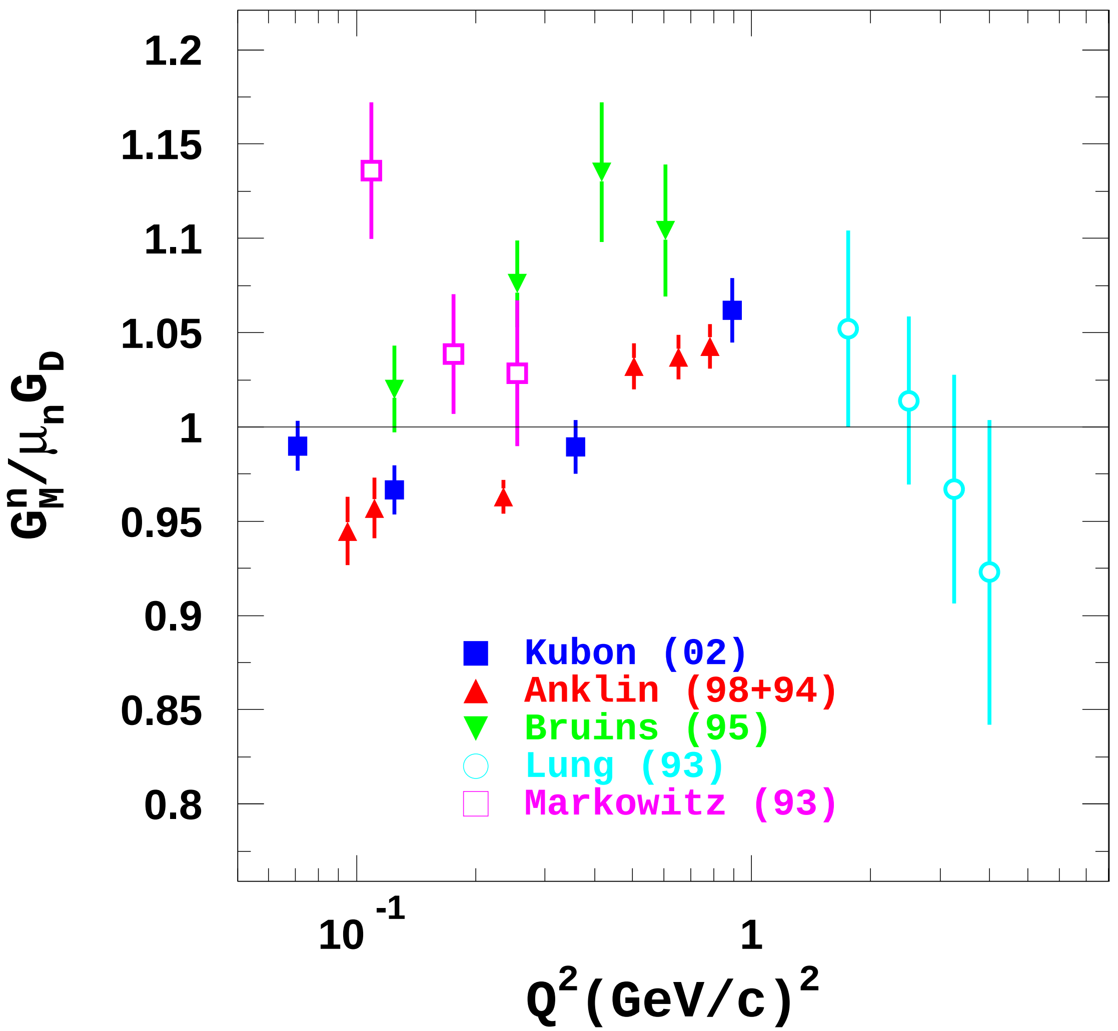

Kubon	ratio
Anklin	ratio
Bruins	ratio
Lung	$D(e,e')X$
Markowitz	$D(e,e'n)p$

$$\text{ratio} \equiv \frac{D(e,e'n)p}{D(e,e'p)n}$$

G_E^n before Polarization

Extract from e-D elastic scattering:

$$\frac{d\sigma}{d\Omega} = \sigma_{NS}\left[A\left(Q^2\right) + B\left(Q^2\right)\tan^2\left(\frac{\theta_e}{2}\right)\right]$$

small θ_e approximation

$$\frac{d\sigma}{d\Omega} = \cdots (G_E^p + G_E^n)^2 \left[u(r)^2 + w(r)^2\right] j_0(\frac{qr}{2})dr \cdots$$

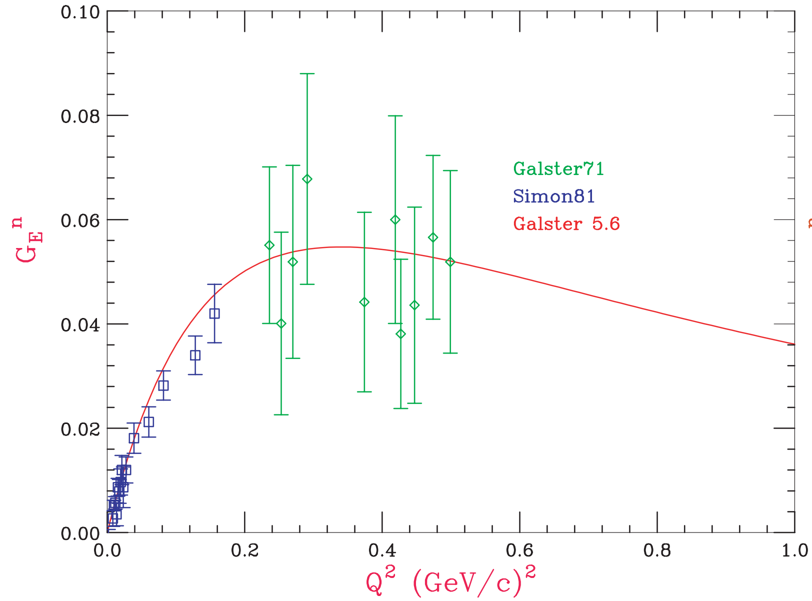

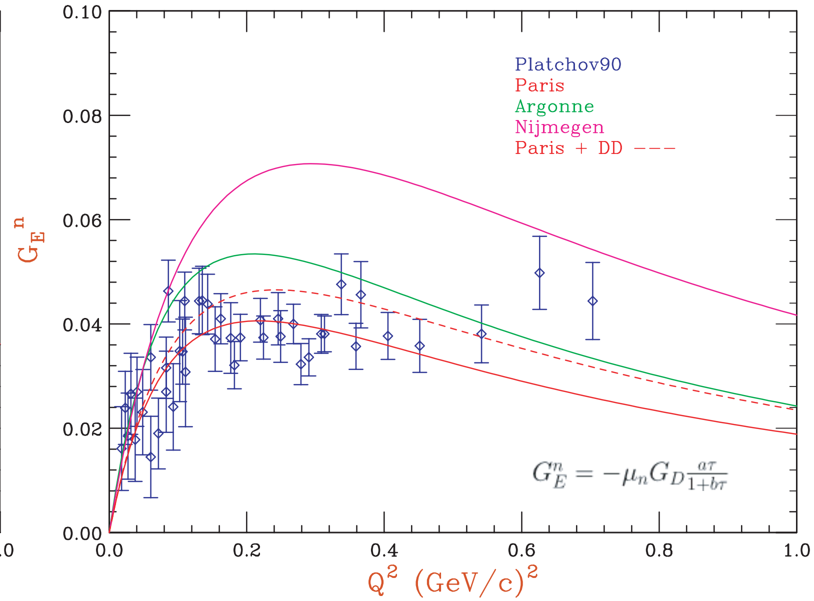

Galster Parametrization: $G_E^n = -\frac{\tau\mu_n}{1+5.6\tau} G_D$ 70's, 80's, & 90's

Notes on e-D

Galster – early 70's   Simon – early 80's   Platchov – early 90's

Elastic $e - D$ scattering at small angles

Neutron–proton interference a plus

Spin-1 ground state: three form factors, G_C , G_Q , G_M

$$A(Q^2) = G_c^2 + \tfrac{8}{9}\eta G_Q^2 + \tfrac{2}{3}\eta^2 G_M^2 \qquad B(Q^2) = \tfrac{4}{3}\eta(\eta+1)G_M^2$$

$$\eta = \tfrac{Q^2}{4M_D^2}$$

$A_{\mathrm{IA}}(Q^2)$ (sum of proton and neutron responses with deuteron wavefunction weighting) deduced after corrections for relativistic effects and MEC

Subtract magnetic dipole using parametrization of data

S and D state functions to unfold nuclear structure for various potentials to get isoscalar form factor

Subtract proton form factor to get G_E^n

Sensitive to deuteron wavefunction model and MEC

Theory&Lattice

Lattice–Quenched QCD Ever since the pioneering numerical simulations of lattice QCD in 1981, the calculation of the light hadron spectrum has been a fundamental subject in lattice QCD. QCD simulations on the lattice, however, require a huge amount of computer time. Therefore, most large scale simulations have been performed using an approximation of neglecting the effects of quark pair-creations and annihilations in the vacuum (quenched approximation). This reduces the computer time by a factor more than 100 and enables QCD simulations on relatively large lattices with high statistics.

Extrapolation of quark massess incorporate the constraints of chiral symmetry

Hank Thacker Donal: Most, if not all, of the calculations of nucleon form factors to date have used what are called Wilson or Wilson-Dirac fermions. This refers to the particular way of discretising the Dirac opeator for quarks on the lattice. The up and down quark masses have a mass of about 4 and 7 MeV respectively, using standard conventions. Wilson fermions work very well for quark masses greater than about 40 or 50 MeV, but by the time you get down to about 30 MeV, the statistics suddenly go all to hell from what is called the "exceptional configuration problem." My collaborators (Bardeen, Duncan, and Eichten) and I were the first ones to diagnose this problem and implement a cure for it. In our recent work, we have been able to get down to quark masses of about 15 to 20 MeV. But up till now, all of our calculations have been focused on chiral symmetry and, specifically, properties of scalar and pseudoscalar mesons. Also, there have been some relatively recent theoretical developments regarding how to put very light quarks on a lattice (keywords: overlap Dirac operator, Ginsparg-Wilson relations). Future calculations of nucleon form factors will certainly use these new light-quark methods and hopefully get much closer to the physical quark masses. There is also an extensive amount of theoretical work on the general problem of "chiral extrapolation", i.e. understanding from a chiral Lagrangian framework how various quantities depend on the quark mass so we can do more believable extrapolations to the physical values. The state of the art in the whole subject of light quark properties in lattice QCD is a rapidly developing subject. Most of the new technology has not been applied to nucleon form factors yet, so vastly improved calculations will certainly be forthcoming. I myself have been focusing more on mesons recently (which are simpler and more directly relevant to chiral symmetry), but baryon structure will certainly be studied at much lighter quark masses in the relatively near future. –Hank

VMD-PQCD: Eq 2 from GK (1085)

$$F_1^{IV} = \left[\frac{m_\rho^2}{m_\rho^2 + Q^2}\frac{g_\rho}{f_\rho} + \left(1 - \frac{g_\rho}{f_\rho}\right)\right] F_1(Q^2)$$

F1,F2 at low Q2 are known from meson physics and have the monopole form. Due to the additonal pwer of q2 in meson propagator it dies out and we are left with the photon nucleon coupling.

Models of Nucleon Form Factors

VMD	$F(Q^2) = \sum_i \frac{C_{\gamma V_i}}{Q^2+M_{V_i}^2} F_{V_i N}(Q^2)$
	breaks down at large Q^2
CBM	Lu, Thomas, Williams (1998)
pQCD	$F_2 \propto F_1 \left(\frac{M}{Q^2}\right)$ helicity conservation
	Counting rules: $F_1 \propto \frac{\alpha_s^2(Q^2)}{Q^4}$
	$Q^2 F_2/F_1 \rightarrow$ constant
	JLAB proton data: $QF_2/F_1 \rightarrow$ constant
Hybrid VMD-pQCD	GK, Lomon
Lattice	Dong .. (1998)
RCQM	point form (Wagenbrunn..)
	light front (Cardarelli ..)
Soliton	Holzwarth
LFCBM	Miller
Helicity non-conservation	pQCD (Ralston..) LF (Miller..)

Theoretical Models

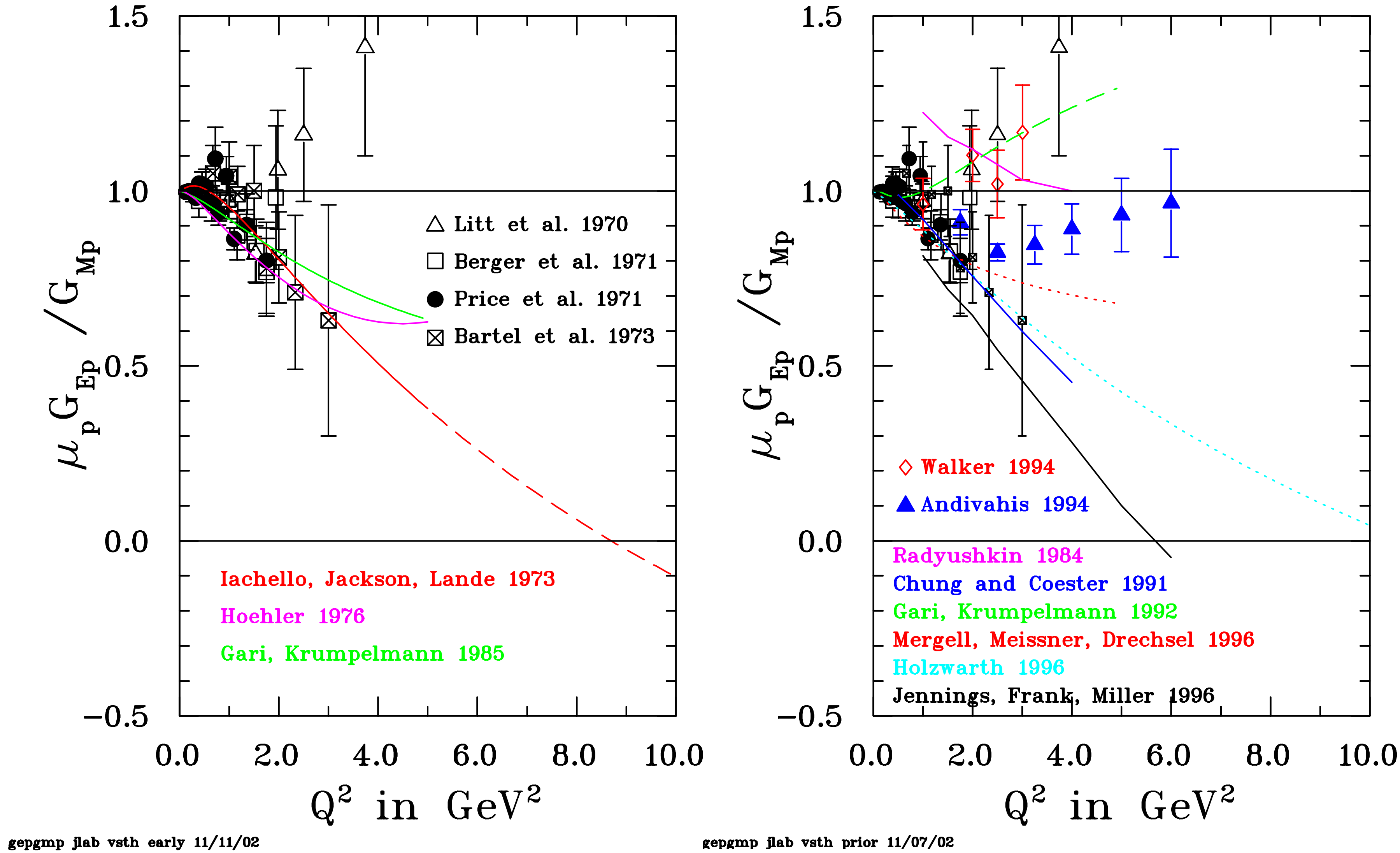

Theoretical Models

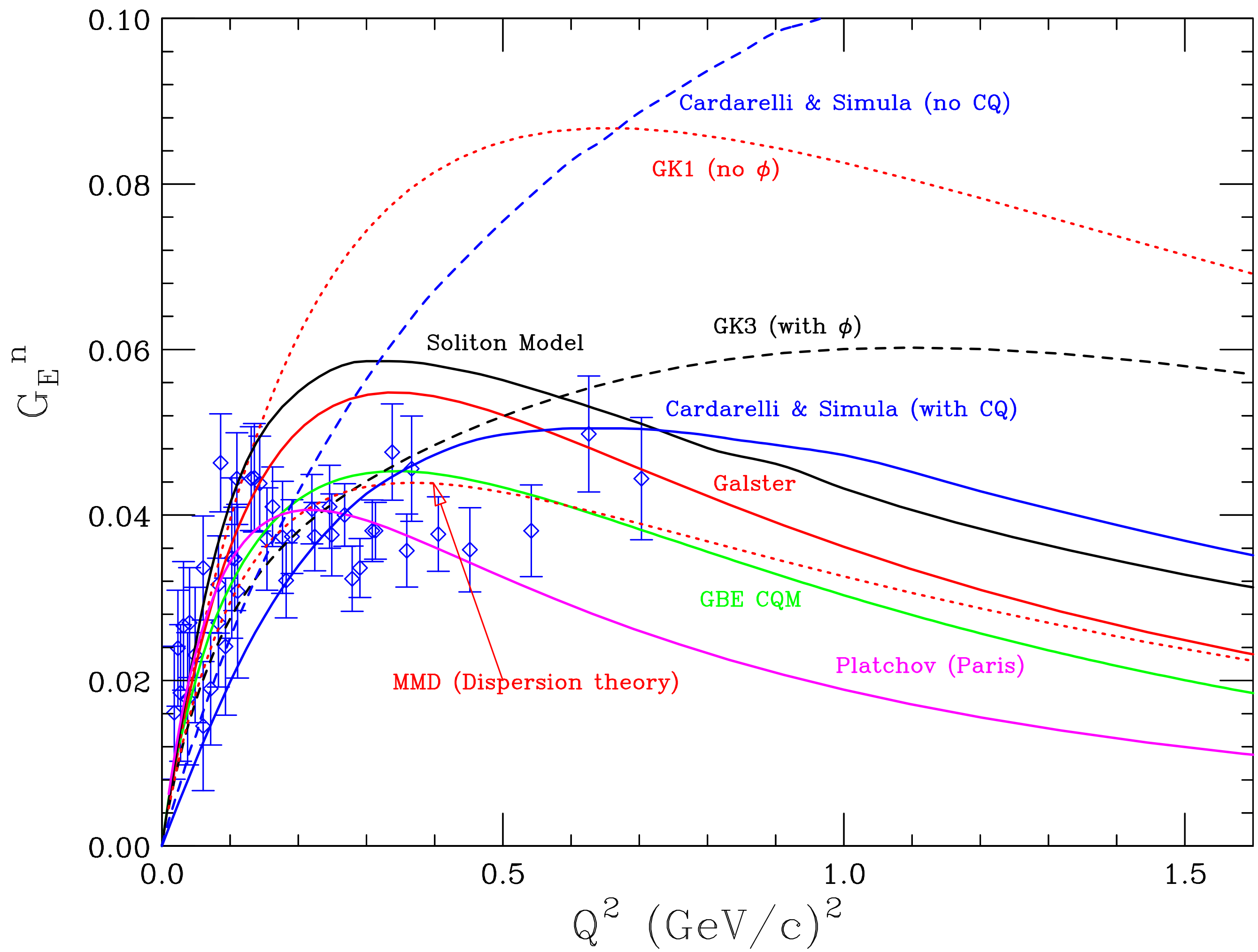

Spin Correlations in elastic scattering

- Dombey, Rev. Mod. Phys. **41** 236 (1968): $\vec{p}(\vec{e}, e')$
- Akheizer and Rekalo, Sov. Phys. Doklady **13** 572 (1968): $p(\vec{e}, e', \vec{p})$
- Arnold, Carlson and Gross, Phys. Rev. C **23** 363 (1981): $^2\mathrm{H}(\vec{e}, e'\vec{n})p$

Essential feature:

$$\frac{d\sigma}{d\Omega} = \underbrace{\ldots(G_E^2 + \ldots G_M^2)}_{(d\sigma/d\Omega)_{\mathrm{unpol}}} + \underbrace{\ldots P_e P_N^{\perp} G_E G_M}_{A_T} + \underbrace{\ldots P_e P_N^{\parallel} G_M^2}_{A_{\parallel}}$$

Early work at Bates, Mainz starting in early 1990's

Spin Correlations

- ✳ Scofield, Phys. Rev. **141** 1352 (1966): all
- ✳ Dombey, Rev. Mod. Phys. **41** 236 (1968): $\vec{p}(\vec{e}, e')$
- ✳ Akheizer and Rekalo, Sov. Phys. Doklady **13** 572 (1968): $p(\vec{e}, e', \vec{p})$
- ✳ Hey and Kabir, Phys. Rev. **187** 1990 (1969): $\vec{p}(e, e', \vec{p})$
- ✳ Arnold, Carlson and Gross, Phys. Rev. C **23** 363 (1981): ${}^{2}\mathrm{H}(\vec{e}, e'\vec{n})p$
- ✳ Blankleider and Woloshyn, Phys. Rev. C **29**, 538 (1984), polarized ^{3}He as an effective polarized neutron
- ✳ Arenhoevel, Leidemann and Tomusiak, Z. Phys. A 331 123 (1988), Polarization Observables in $d(e, e'n)p$

Recoil Polarization

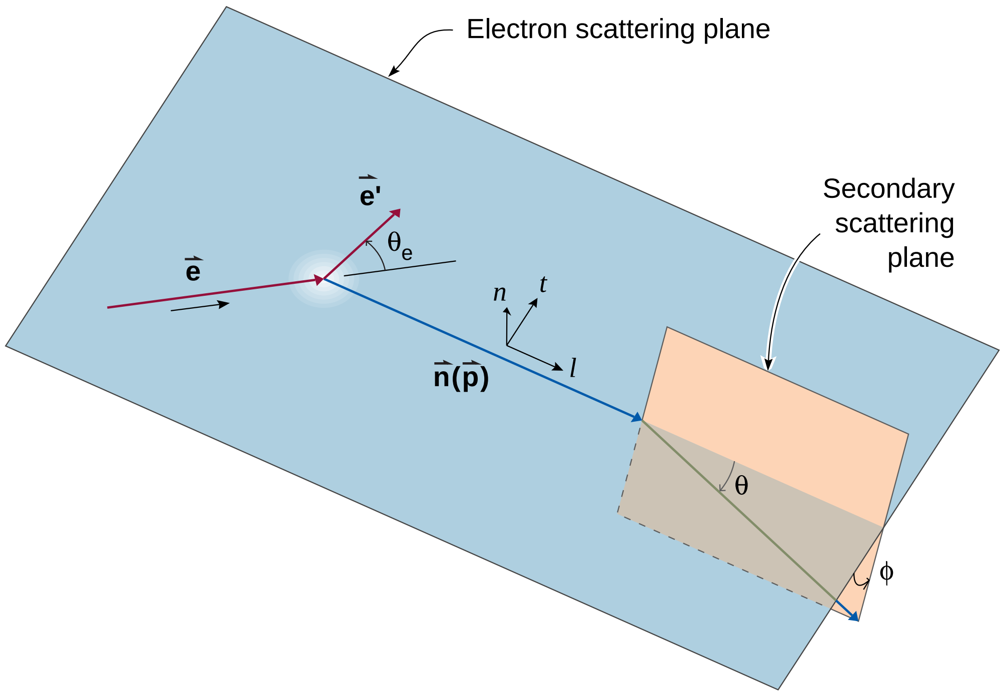

$$I_0 P_t = -2\sqrt{\tau(1+\tau)}\,G_E G_M \tan(\theta_e/2)$$
$$I_0 P_l = \frac{1}{M_N}(E_e + E_{e'})\sqrt{\tau(1+\tau)}\,G_M^2 \tan^2(\theta_e/2)$$

$$\boxed{\frac{G_E}{G_M} = -\frac{P_t}{P_l}\frac{(E_e+E_{e'})}{2M_N}\tan\left(\frac{\theta_e}{2}\right)}$$

Direct measurement of form factor ratio by measuring the ratio of the transfered polarization P_t and P_l

Recoil

In elastic scattering of polarized electrons from a nucleon, the recoil nucleon obtains P_l and P_t sensitive to $G_E \cdot G_M$ and G_M^2 respectively.

Elastic scattering of polarised nucleons on unpolarised protons has analysing power $\epsilon(\theta_n)$ due to spin-orbit term V_{LS} in NN interaction:

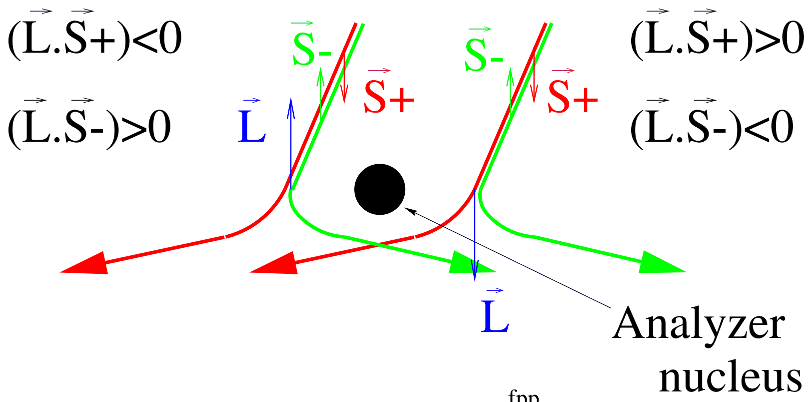

If more S+ than S- $(+P^{fpp})$ ...

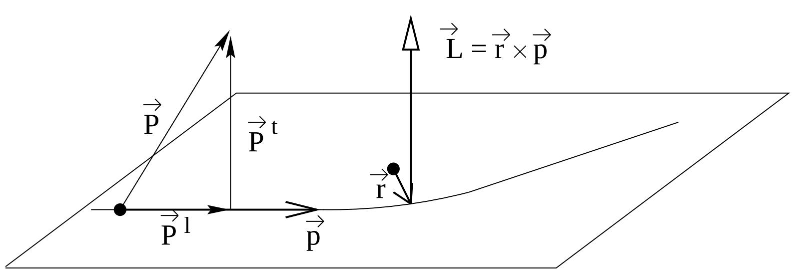

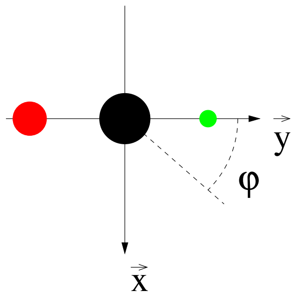

... more events left than right

Left-right asymmetry is observed if the proton is polarized vertically, strong interaction with analyzer nucleus depends on its spin.

Recoil Polarization – Principle and Practice

- Interested in transfered polarization, P_l and P_t, at the target
- Polarimeters are sensitive to the perpendicular components only, $P_n^{\rm pol}$ and $P_t^{\rm pol}$

  Measuring the ratio P_t/P_l requires the precession of P_l by angle χ before the polarimeter.
- If polarization precesses χ (e.g. in a dipole):
  $P_n^{\rm pol} = \sin\chi \cdot hP_l$ and $P_t^{\rm pol} = hP_t$

  $P_t^{\rm pol} = P_t$ in scattering plane and proportional to $G_E G_M$

  $P_n^{\rm pol}$ is related to G_M^2
- G_E^p/G_M^p via ${}^1{\rm H}(\vec{e}, e'\vec{p})$ at Jefferson Lab and Mainz
- G_E^n/G_M^n via ${}^2{\rm H}(\vec{e}, e'\vec{n})p$ at Jefferson Lab and Mainz

Quality of polarimeter data optimized by taking advantage of proper flips (helicity reversals).

$$L_1 = N_o[1 + pA_y(\theta + \alpha)]$$
$$R_2 = N_o[1 - pA_y(\theta + \beta)]$$
$$R_1 = N_o[1 - pA_y(\theta + \alpha)]$$
$$L_2 = N_o[1 + pA_y(\theta + \beta)]$$

Using the geometric means, $L \equiv \sqrt{L_1 L_2} \text{and} R \equiv \sqrt{R_1 R_2}$, the false (instrumental) asymmetries, α and β, cancel.

$$\xi = pA_y = \frac{L - R}{L + R}$$

G_E^p at Jefferson Lab (Hall A)

$\boxed{\text{E93-027 (data taken in 1998)}}$

Jones *et al.*, PRL 84, 1398 (2000)

* G_E^p/G_M^p out to $Q^2 = 3.5\ \mathrm{GeV/c^2}$
* Electron in one HRS and proton in FPP in other HRS

$\boxed{\text{E99-007 (data taken in 2000)}}$

Gayou *et al.* PRL 88, 092301 (2002)

* G_E^p/G_M^p out to $Q^2 = 5.6\ \mathrm{GeV/c^2}$
* electron in one spectrometer and proton in FPP in other
* above $Q^2 = 3.5$ proton in FPP in one spectrometer and electron in calorimeter.

G_E^p at Jefferson Lab (Hall A)

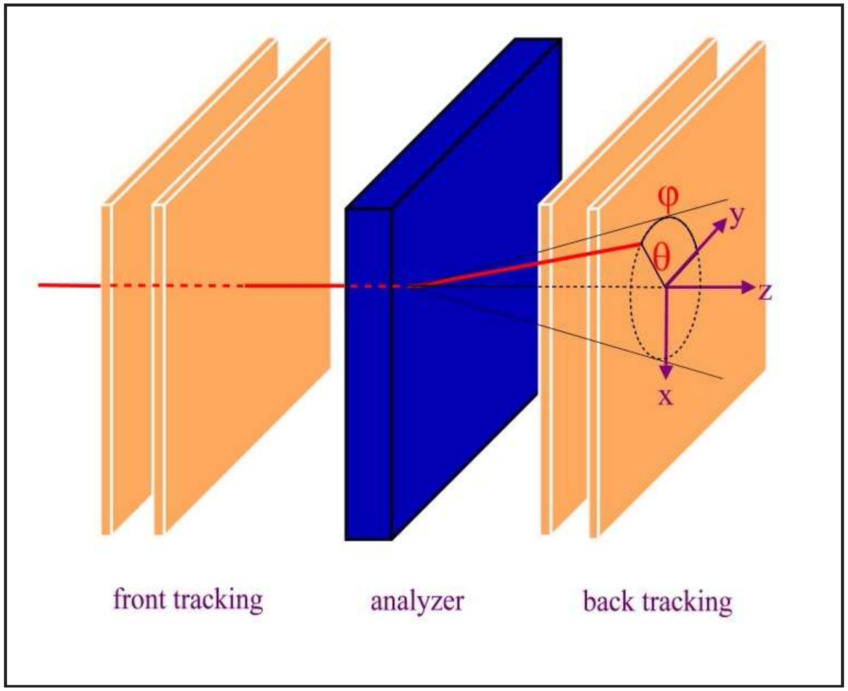

- ✴ left–right asymmetry $\Rightarrow P_n^{\text{fpp}}$ polarization in vertical direction
- ✴ up–down asymmetry $\Rightarrow P_t^{\text{fpp}}$ polarization in the horizontal direction

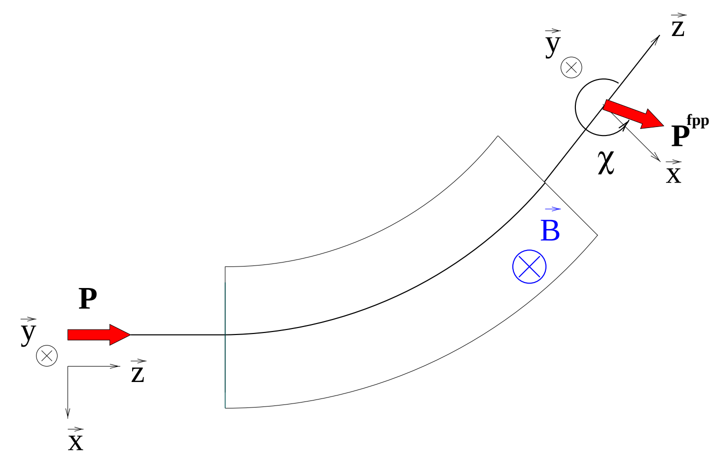

$$P_n^{\text{fpp}} = \sin\chi \cdot hP_l$$
$$P_t^{\text{fpp}} = hP_t$$
$$\chi = \gamma\theta_B(\mu_p - 1)$$

G_E^p in Hall A

Azimuthal Distribution

$$N(\vartheta,\varphi) = N_0(\vartheta)\epsilon(\vartheta)\left\{1 + \left[hA_y(\vartheta)P_t^{\mathrm{fpp}} + a_{\mathrm{instr}}\right]\sin\varphi - \left[hA_y(\vartheta)P_n^{\mathrm{fpp}} + b_{\mathrm{instr}}\right]\cos\varphi\right\}$$

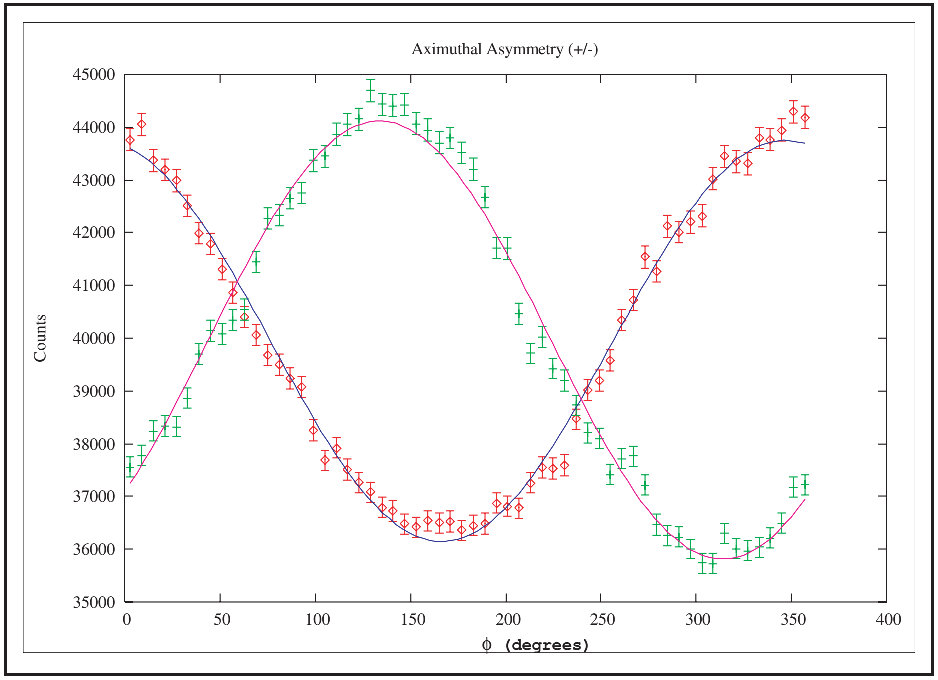

* Difference between 2 helicity states
  - instrumental asymmetries cancel, P_B and A_y cancel.
  - gain access to the polarization components

G_E^p in Hall A

Difference between 2 helicity states ($Q^2 = 5.6$)

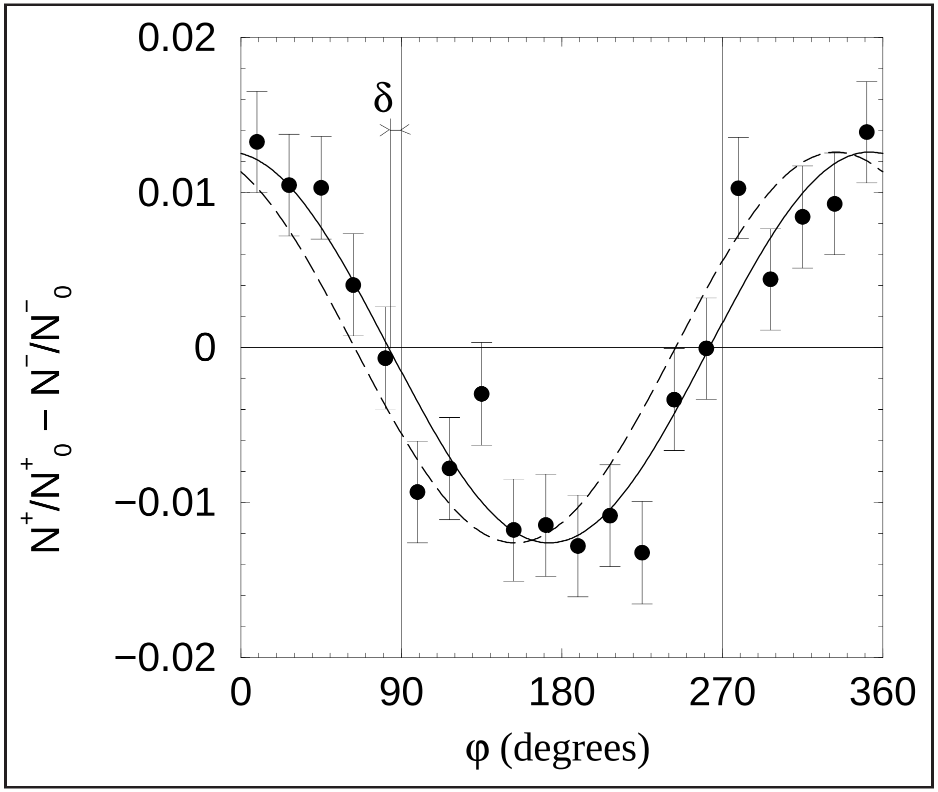

- ✷ Fit $N^+ - N^-$ with $F(\varphi) = C\cos(\varphi + \delta) \rightarrow \tan\delta = P_t^{\text{fpp}}/P_n^{\text{fpp}} \simeq 7^\circ$
- ✷ $P_n^{\text{fpp}} = \sin\chi \cdot hP_l, \qquad P_t^{\text{fpp}} = hP_t$
- ✷ $\frac{G_E}{G_M} = -\frac{P_t}{P_l}\frac{(E_e + E_{e'})}{2M_N}\tan(\frac{\theta_e}{2})$

G_E^p in Hall A – Results

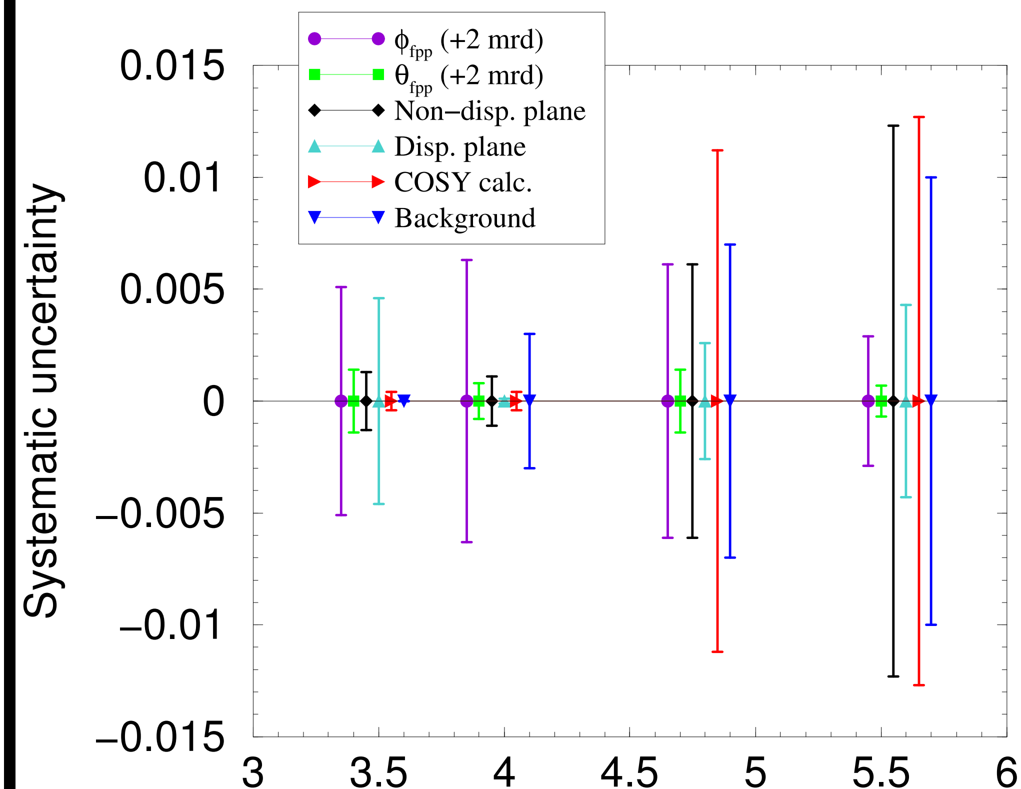

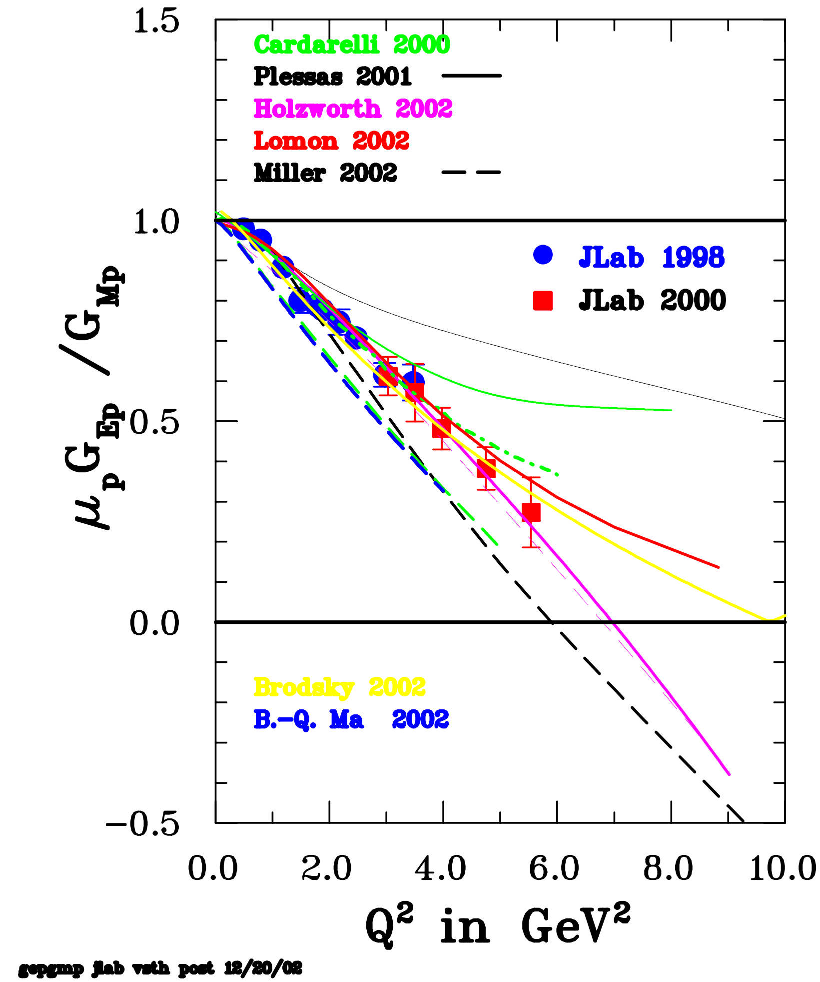

G_E^p in Hall A – Results

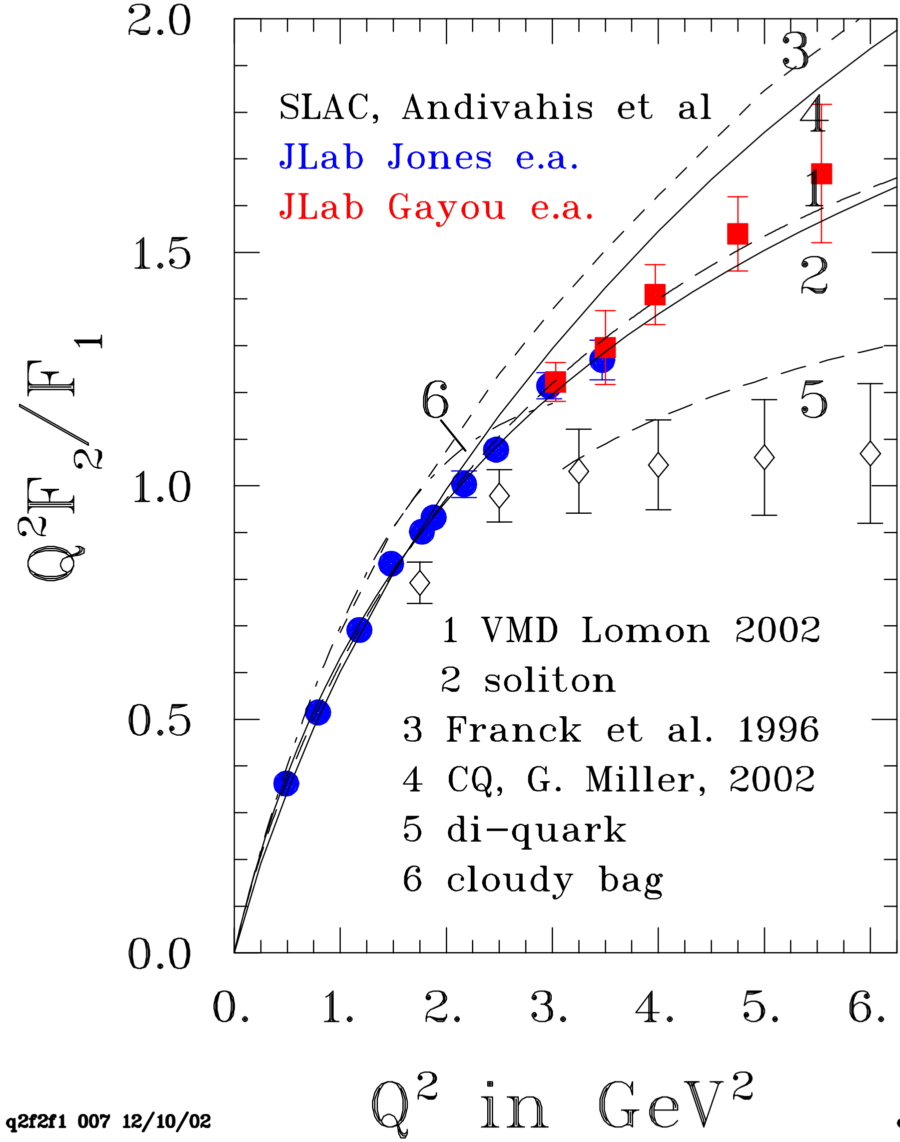

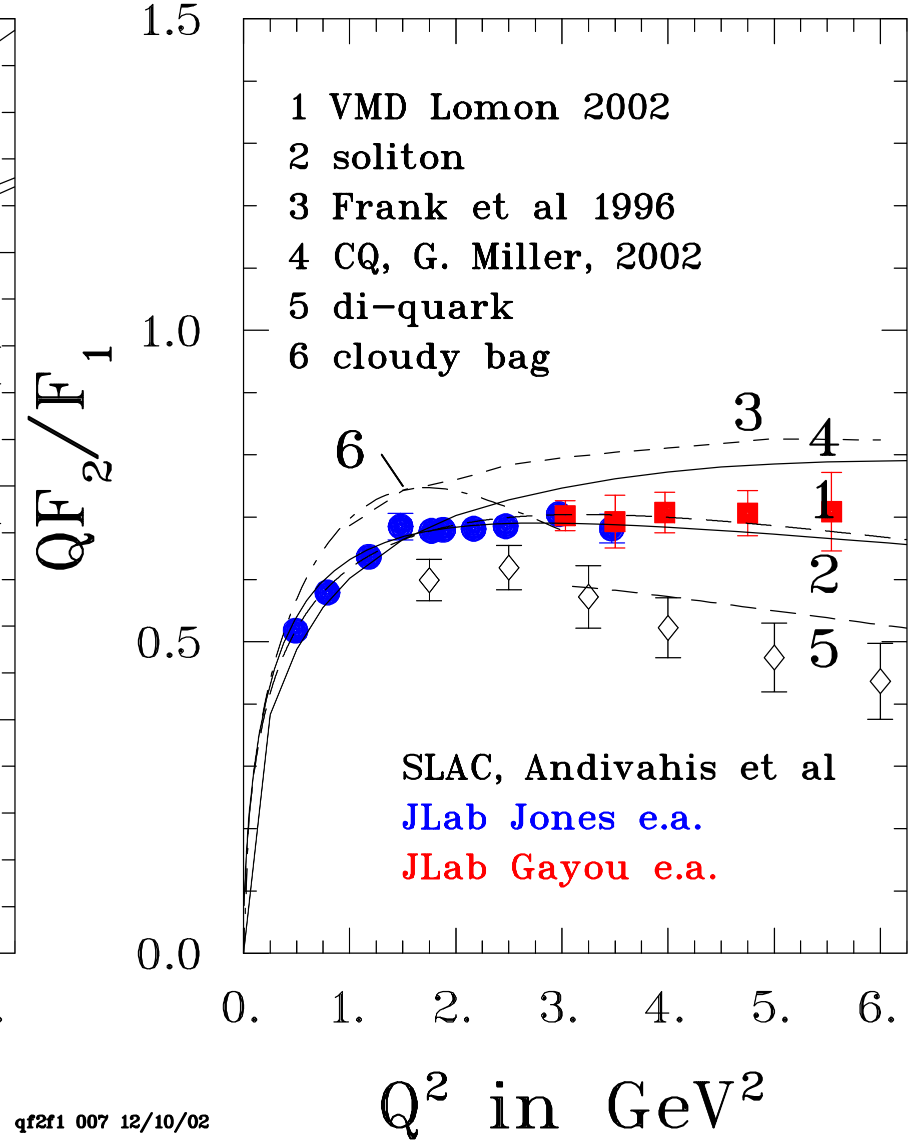

Polarization Experiments on the Neutron

Laboratory	Collaboration	$Q^2 (\mathrm{GeV/c})^2$	Reaction	Reported
MIT-Bates	E85-05	0.255	$^{2}\mathrm{H}(\tilde{\mathrm{e}}, \mathrm{e}'\tilde{\mathrm{n}})$	1994
	BLAST	0.1–0.8	$^{2}\tilde{\mathrm{H}}(\tilde{\mathrm{e}}, \mathrm{e}'\mathrm{n})$	2004
Mainz-MAMI	A3	0.31	$^{3}\tilde{\mathrm{He}}(\tilde{\mathrm{e}}, \mathrm{e}'\mathrm{n})$	1994
	A3	0.15, 0.34	$^{2}\mathrm{H}(\tilde{\mathrm{e}}, \mathrm{e}'\tilde{\mathrm{n}})$	1999
	A3	0.385	$^{3}\tilde{\mathrm{He}}(\tilde{\mathrm{e}}, \mathrm{e}'\mathrm{n})$	1999
	A1	0.67	$^{3}\tilde{\mathrm{He}}(\tilde{\mathrm{e}}, \mathrm{e}'\mathrm{n})$	1999/2003
	A1	0.3, 0.6, 0.8	$^{2}\mathrm{H}(\tilde{\mathrm{e}}, \mathrm{e}'\tilde{\mathrm{n}})$	in 2004
NIKHEF		0.21	$^{2}\tilde{\mathrm{H}}(\tilde{\mathrm{e}}, \mathrm{e}'\mathrm{n})$	1999
Jefferson Lab	E93026	0.5, 1.0	$^{2}\tilde{\mathrm{H}}(\tilde{\mathrm{e}}, \mathrm{e}'\mathrm{n})$	2001/2004
	E93038	0.45, 1.15, 1.47	$^{2}\mathrm{H}(\tilde{\mathrm{e}}, \mathrm{e}'\tilde{\mathrm{n}})$	2003

G_E^n through recoil polarization

Recoil polarization, ${}^2\mathrm{H}(\vec{e}, e'\vec{n})p$, Mainz & JLAB

- ✳ In quasifree kinematics, $P_{s'}$ is sensitive to G_E^n and insensitive to nuclear physics
- ✳ Up–down asymmetry $\xi \Rightarrow$ transverse (sideways) polarization $P_{s'} = \xi_{s'}/P_e A_{\mathrm{pol}}$. Requires knowledge of P_e and A_{pol}
- ✳ Rotate the polarization vector in the scattering plane (with dipole magnet) and measure the longitudinal polarization, $P_{l'} = \xi_{l'}/P_e A_{\mathrm{pol}}$
- ✳ Take ratio, $\frac{P_{s'}}{P_{l'}}$. P_e and A_{pol} cancel
- ✳ E93038 at JLAB's Hall C: Three momentum transfers, $Q^2 = 0.45, 1.13,$ and $1.45 (\mathrm{GeV/c})^2$. Data taking 2000/2001
- ✳ See talk by

Notes on Extraction of the neutron form factors

No free neutron targets – scattering from a nucleus, D, ^{3}He

Neutron is not free - can not avoid engaging the details of the nuclear physics.

Minimize sensitivity to the how the reaction is treated and maximize the sensitivity to the neutron form factors by working in quasifree kinematics.

- ✳ Indirect measurements: The experimental asymmetries ($\xi_{s'}$, A_V^{ed}, $A_{\exp}^{qe}$) are compared to theoretical calculations.
- ✳ Theoretical calculations are generated for scaled values of the form factor.
- ✳ Form factor is extracted by comparison of the experimental asymmetry to acceptance averaged theory.

G_E^n in Hall C via $^2\mathrm{H}(\vec{e}, e'\vec{n})p$

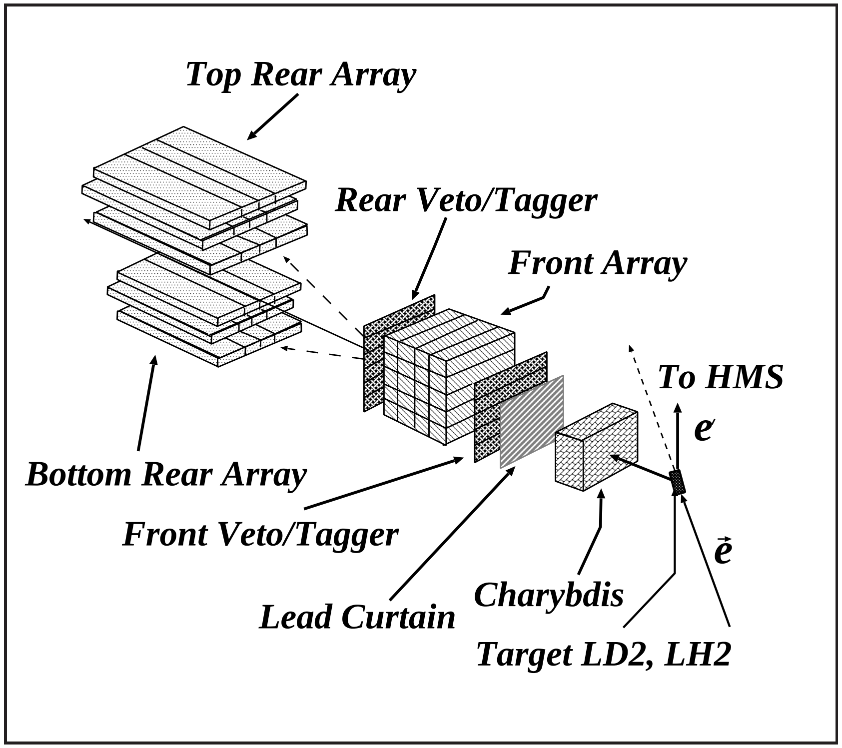

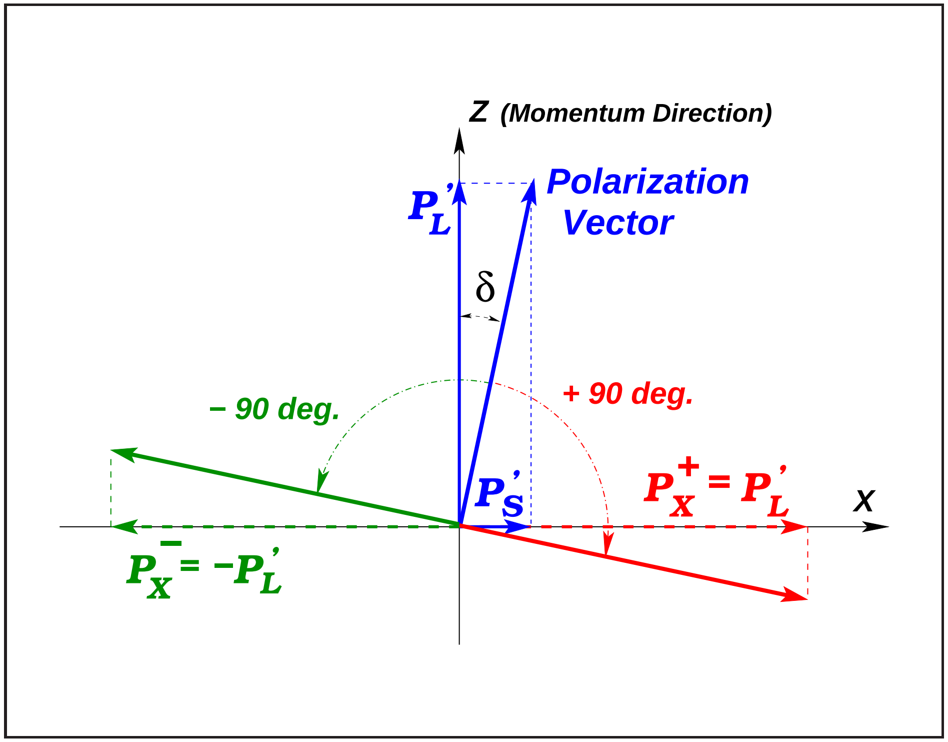

Taking the ratio eliminates the dependence on the analyzing power and the beam polarization → greatly reduced systematics

$$\frac{G_E^n}{G_M^n} = K \tan\delta \qquad \text{where} \qquad \tan\delta = \frac{P_{s'}}{P_{l'}} = \frac{\xi_{s'}}{\xi_{l'}}$$

Notes on recoil polarimeter

Neutron Recoil Polarization at JLab E93-038, Madey et al.

Dipole magnet for spin precession

Lead curtain suppresses background

Front tagger identifies charged particles

4x5 front array detects nucleon

Rear tagger distinguishes (n,n) from (n,p)

Segmentation permits tracking

Up/down asymmetry measures sideways polarization

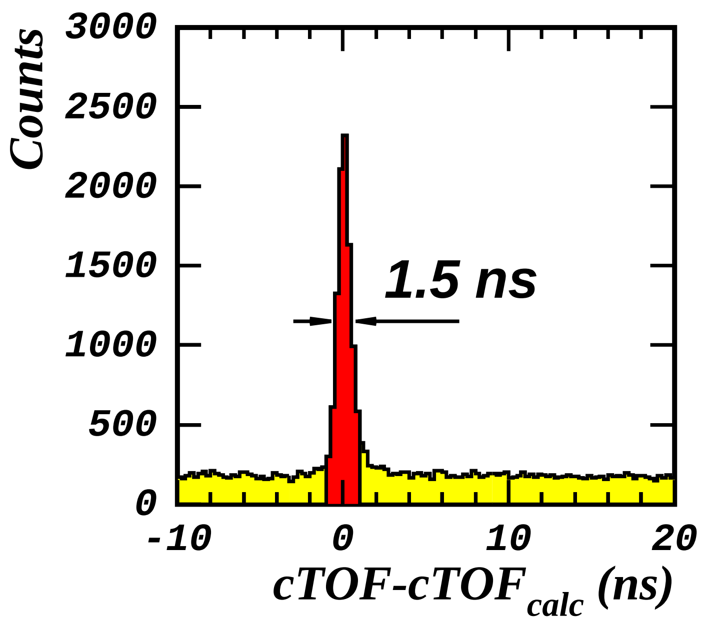

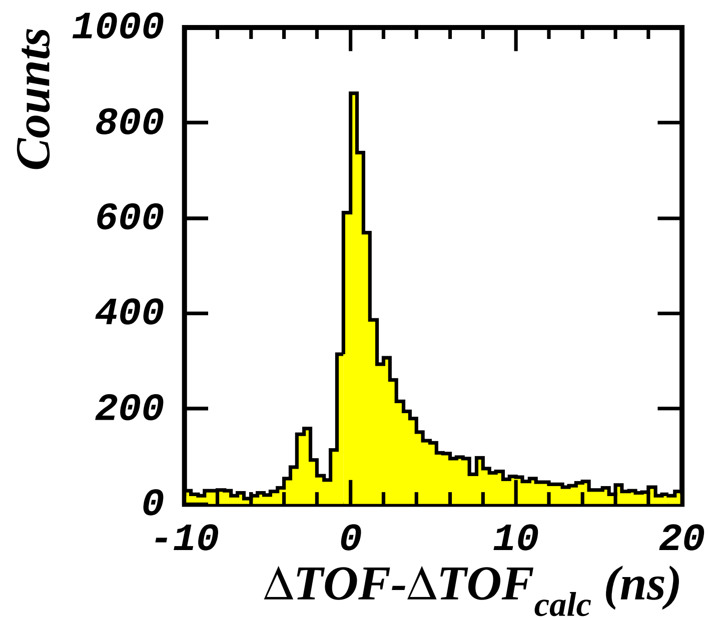

Left: Coincidence TOF for neutrons. Difference between measured TOF and calculated TOF assuming quasi-elastic neutron. Right: ΔTOF for neutron in front array and neutron in rear array.

ΔTOF is kept as the four combinations of (-,+) helicity, and (Upper,Lower) detector and cross ratios formed. False asymmetries cancel.

$$r = \left(\frac{N_U^+ N_D^-}{N_U^- N_D^+} \right)^{1/2} \qquad \xi = (r-1)/(r+1)$$

G_E^n in Hall C via ${}^2\mathrm{H}(\vec{e}, e'\vec{n})p$

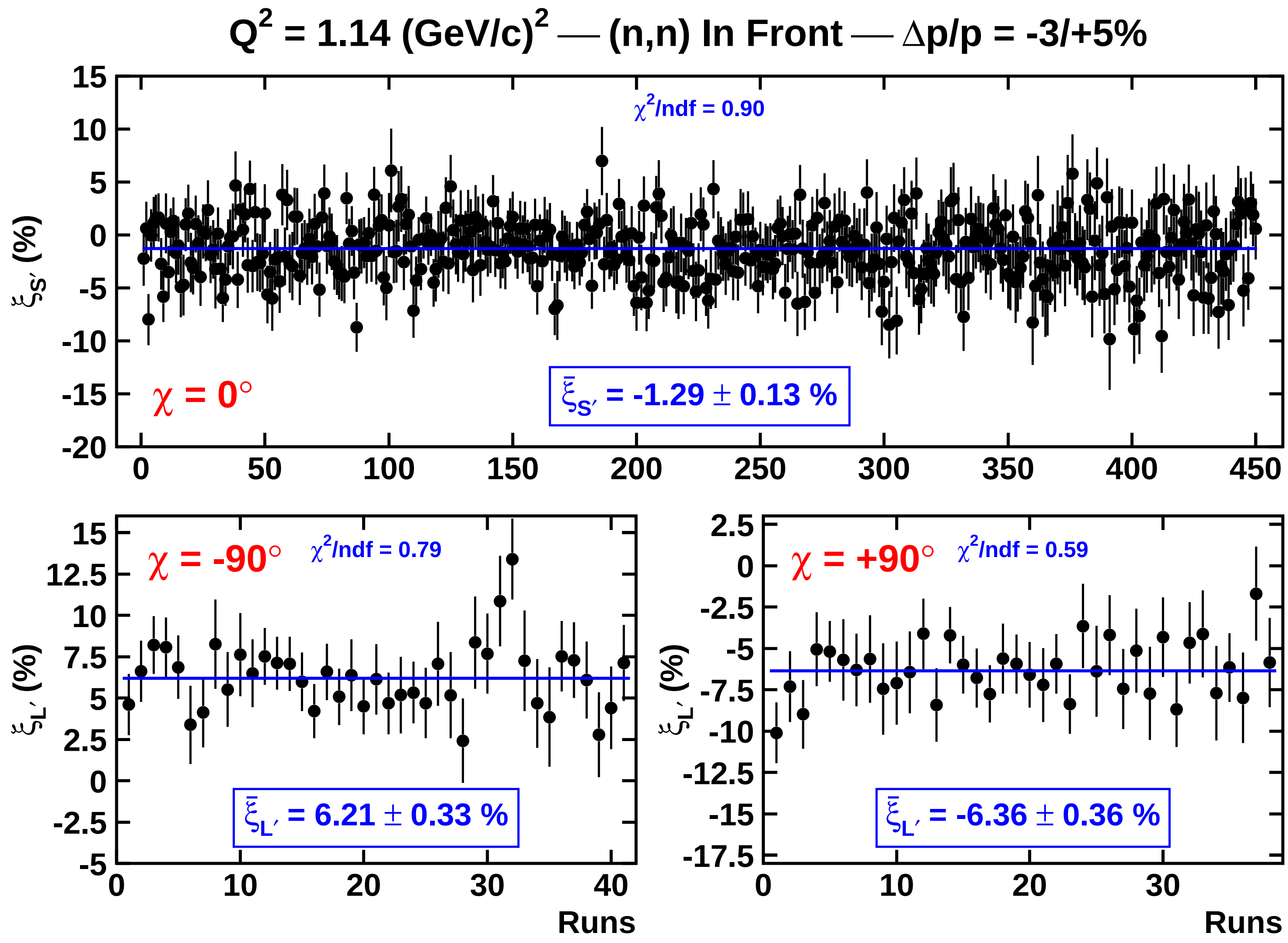

G_E^n in Hall C via ${}^2\mathrm{H}(\vec{e}, e'\vec{n})p$

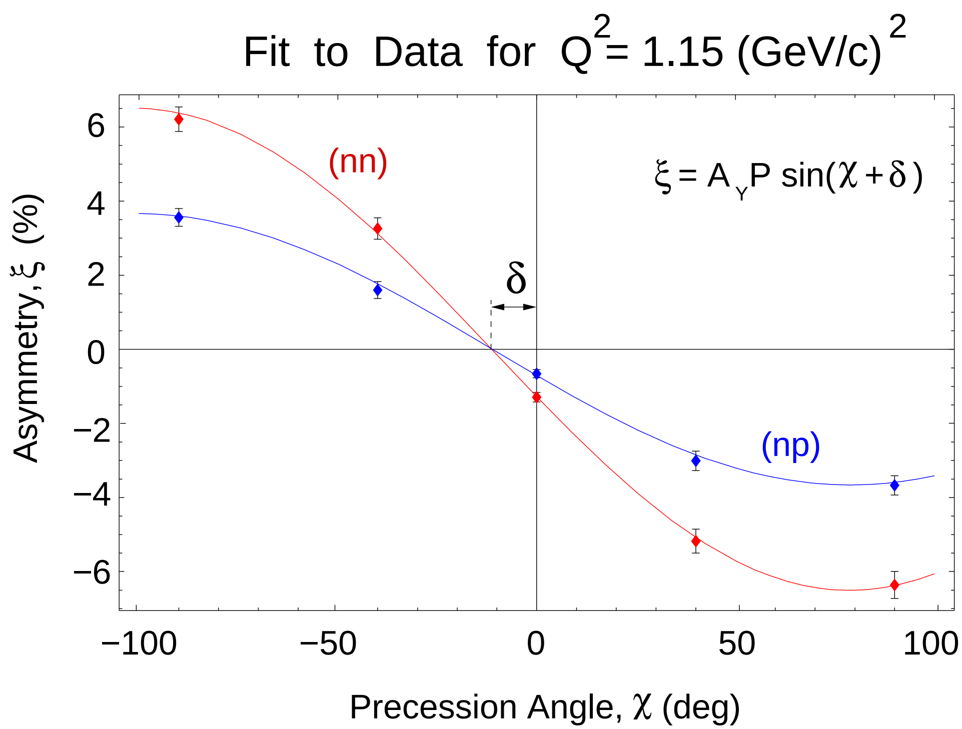

$$\xi \propto \sin(\chi + \delta) \Rightarrow g = \frac{G_E^n}{G_M^n} = -\tan\delta\sqrt{\frac{\tau(1+\epsilon)}{2\epsilon}}$$

G_E^n via ${}^2\mathrm{H}(\vec{e}, e'\vec{n})p$

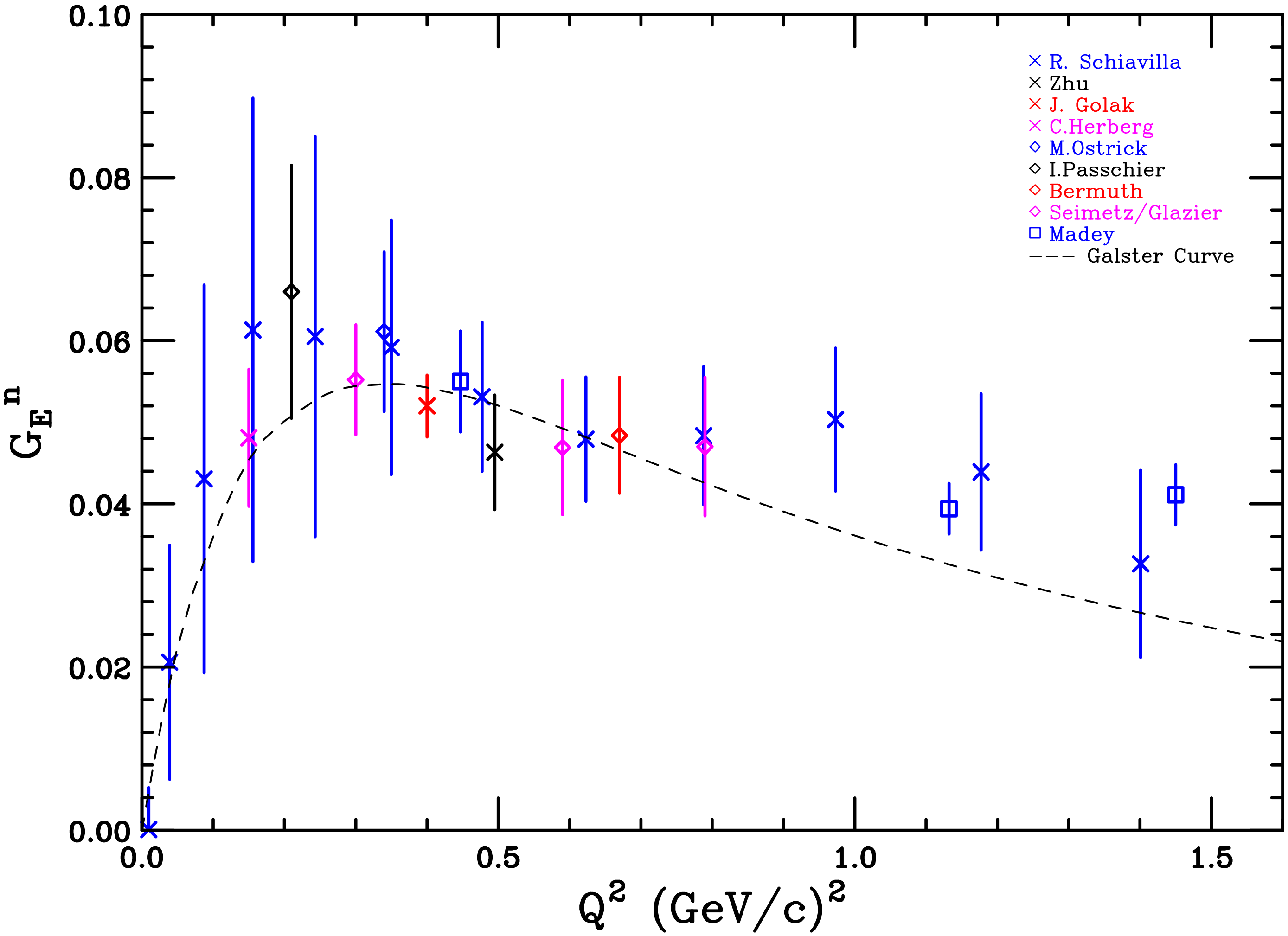

Beam–Target Asymmetry - Principle

Polarized Cross Section:

$\sigma = \Sigma + h\Delta$

Beam Helicity $h \pm 1$

$$A = \frac{\sigma_+ - \sigma_-}{\sigma_+ + \sigma_-} = \frac{\Delta}{\Sigma}$$

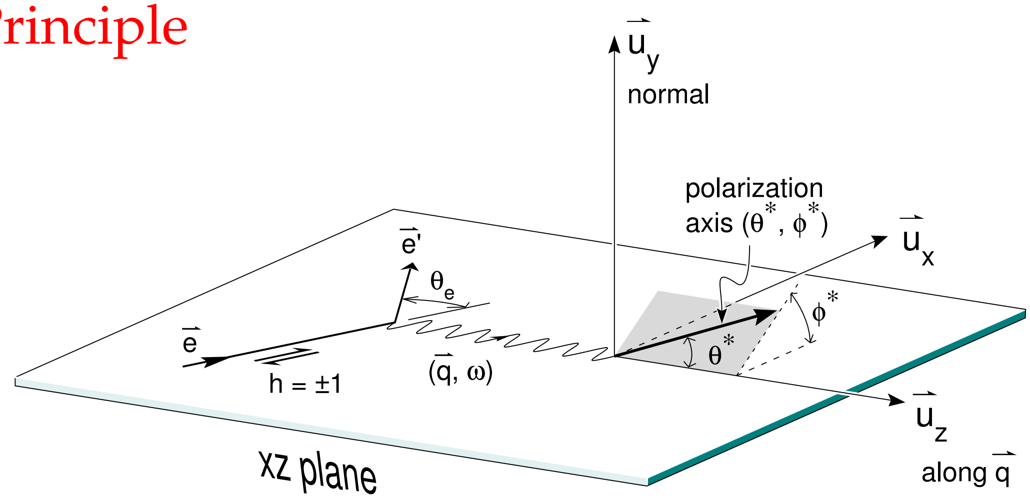

$$A = \frac{\overbrace{a\cos\Theta^\star (G_M)^2}^{A_T} + \overbrace{b\sin\Theta^\star\cos\Phi^\star G_E G_M}^{A_{TL}}}{c\,(G_M)^2 + d\,(G_E)^2}; \quad \varepsilon = \frac{N^\uparrow - N^\downarrow}{N^\uparrow + N^\downarrow} = P_B \cdot P_T \cdot f \cdot A$$

$$\boxed{\begin{array}{l}\Theta^\star = 90^\circ \quad \Phi^\star = 0^\circ \\ \Longrightarrow A_{TL} = \dfrac{b G_E G_M}{c\,(G_M)^2 + d\,(G_E)^2}\end{array}}$$

$$\boxed{\begin{array}{l}\Theta^\star = 0^\circ \quad \Phi^\star = 0^\circ \\ \Longrightarrow A_T = \dfrac{a G_M^2}{c\,(G_M)^2 + d\,(G_E)^2}\end{array}}$$

$\overrightarrow{^3\mathrm{He}}$, $\overrightarrow{^2\mathrm{H}}$

Beam–Target Asymmetry - Practice

- ✳ No free neutron
- ✳ Unpolarized materials
- ✳ Protons dominate
- ✳ The deuteron and ^{3}He only approximate a polarized neutron
- ✳ Scattering from other polarized materials
- ✳ Indirect measurement of form factors
- ✳ Taking ratio of A_{TL}/A_T not always practical; errors arising from P_t and P_b

E93-026 $\overrightarrow{\mathrm{D}}(\vec{e}, e'n)p$ $\boxed{\sigma(h,P) = \sigma_0\left(1 + hPA^V_{ed}\right)}$

A^V_{ed} is sensitive to G^n_E

has low sensitivity to potential models

has low sensitivity to subnuclear degrees of freedom (MEC, IC)

in quasielastic kinematics

Sensitivity to G^n_E – Insensitivity to Reaction

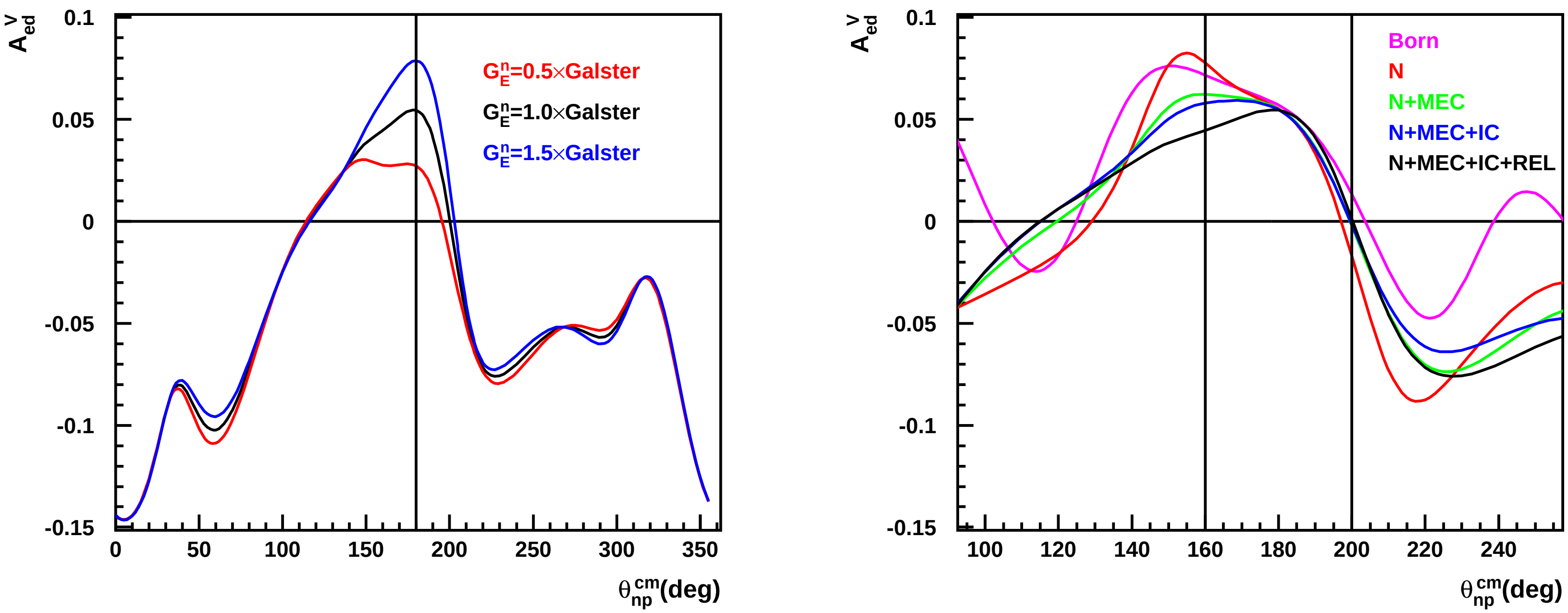

G_E^n in Hall C

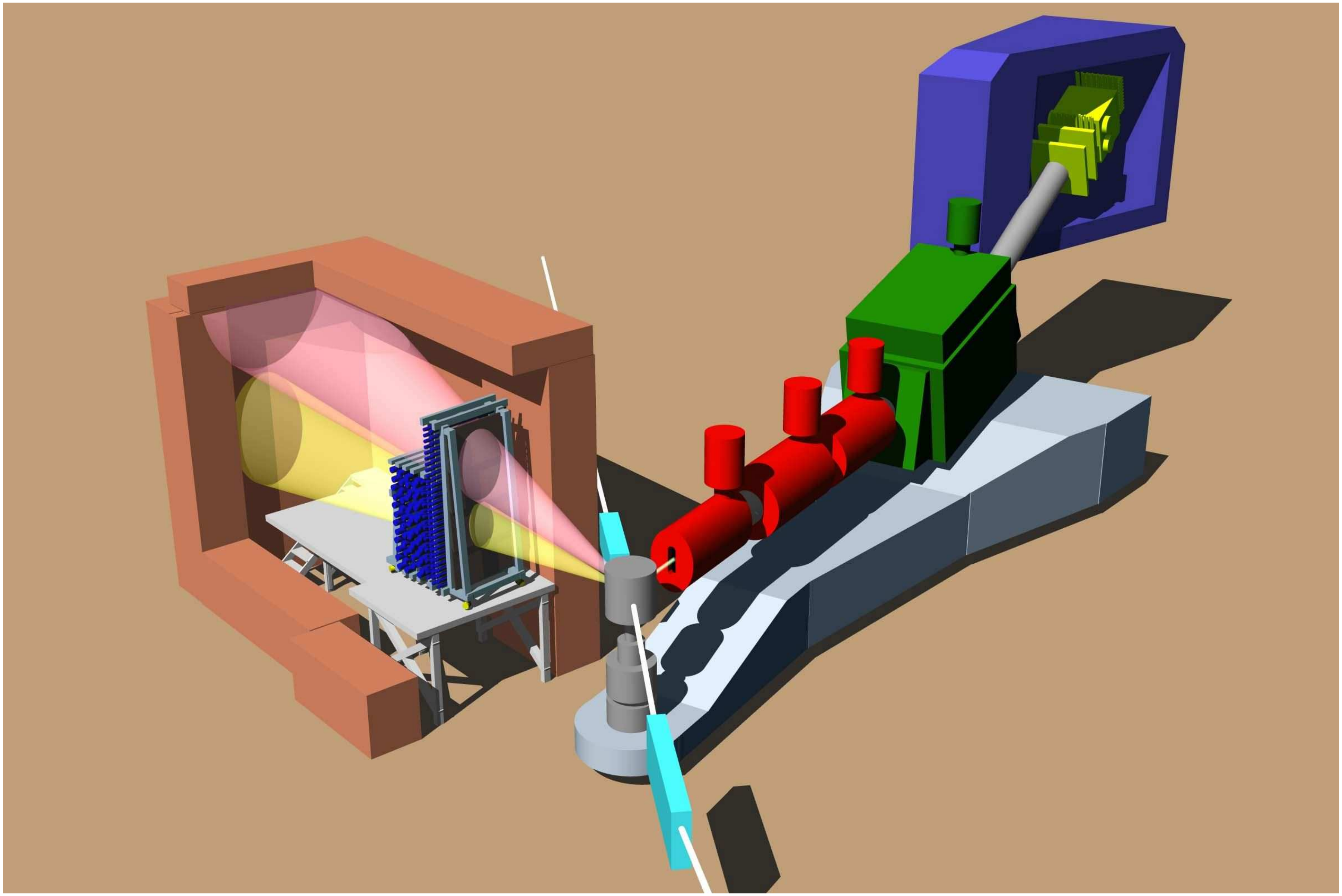

Notes on Hall C Setup

- ✳ Polarized Target
- ✳ Chicane to compensate for beam deflection of ≈ 4 degrees
- ✳ Scattering Plane Tilted
- ✳ Protons deflected ≈ 17 deg at $Q^2 = 0.5$
- ✳ Raster to distribute beam over 3 cm^2 face of target
- ✳ Electrons detected in HMS (right)
- ✳ Neutrons and Protons detected in scintillator array (left)
- ✳ Beam Polarization measured in coincidence Möller polarimeter

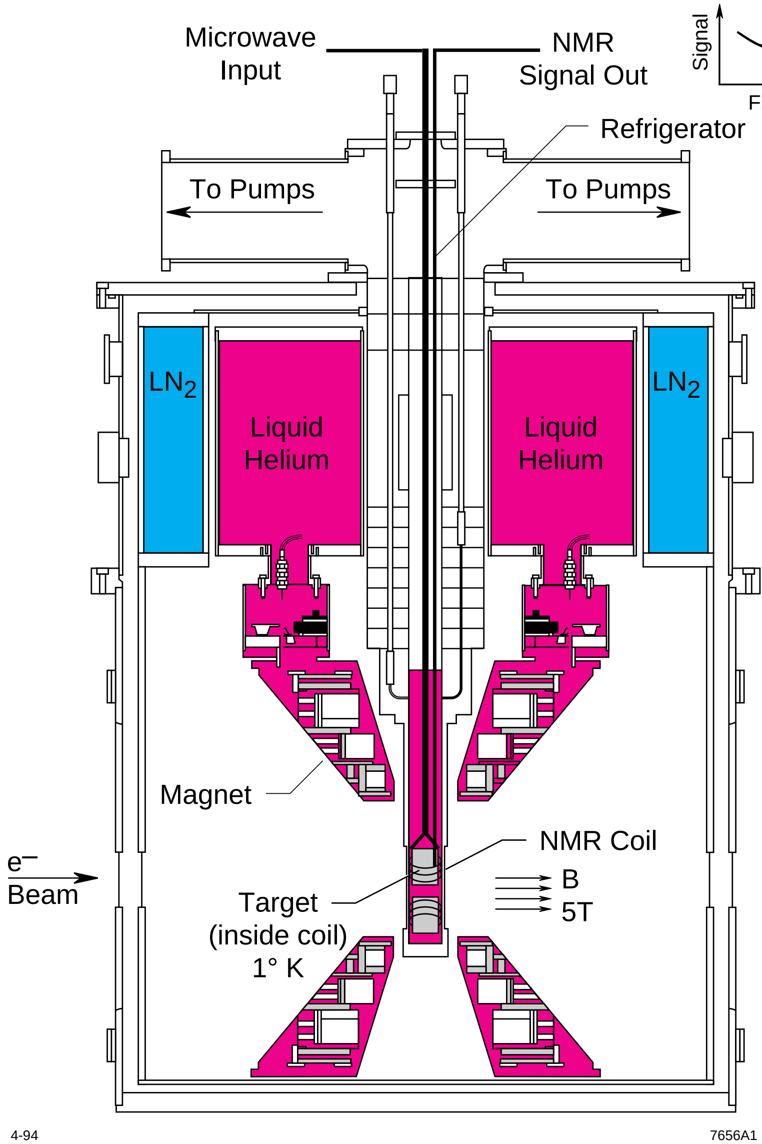

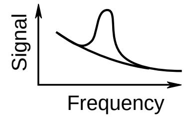

Solid Polarized Targets

- ✳ frozen(doped) $^{15}ND_3$
- ✳ ^{4}He evaporation refrigerator
- ✳ $5T$ polarizing field
- ✳ remotely movable insert
- ✳ dynamic nuclear polarization

Polarized Target

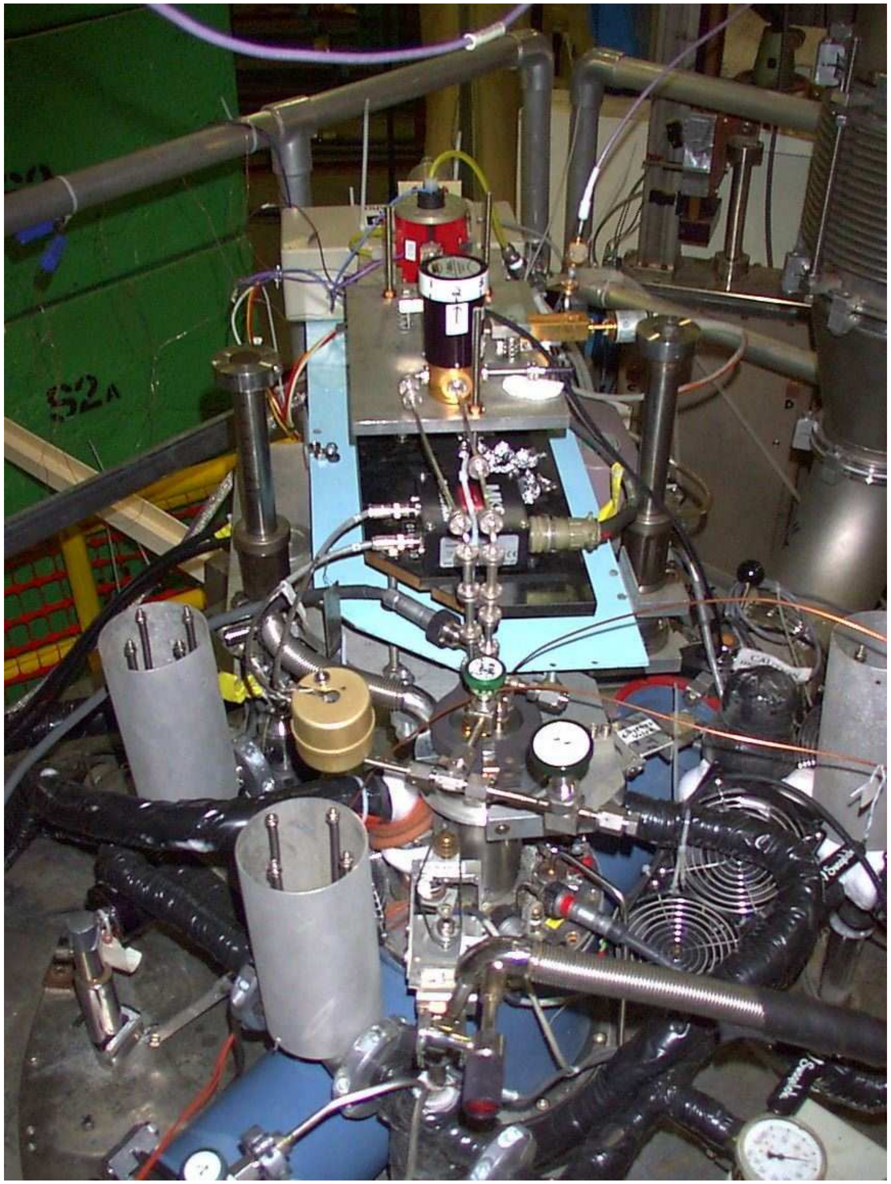

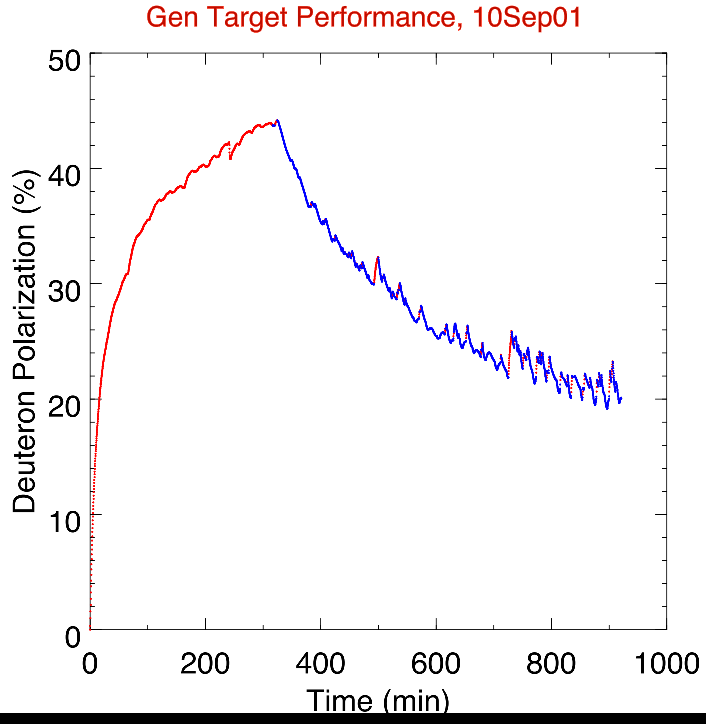
Gen Target Performance, 10Sep01
Deuteron Polarization (%)
Time (min)
0
10
20
30
40
50
0
200
400
600
800
1000

Neutron Detector

- ✳ Highly segmented scintillator
- ✳ Rates: 50 - 200 kHz per detector
- ✳ Pb shielding in front to reduce background
- ✳ 2 thin planes for particle ID (VETO)
- ✳ 6 thick conversion planes
- ✳ 142 elements total, >280 channels
- ✳ Extended front section for symmetric proton coverage
- ✳ PMTs on both ends of scintillator
- ✳ Spatial resolution $\simeq$ 10 cm
- ✳ Time resolution $\simeq$ 400 ps
- ✳ Provides 3 space coordinates, time and energy

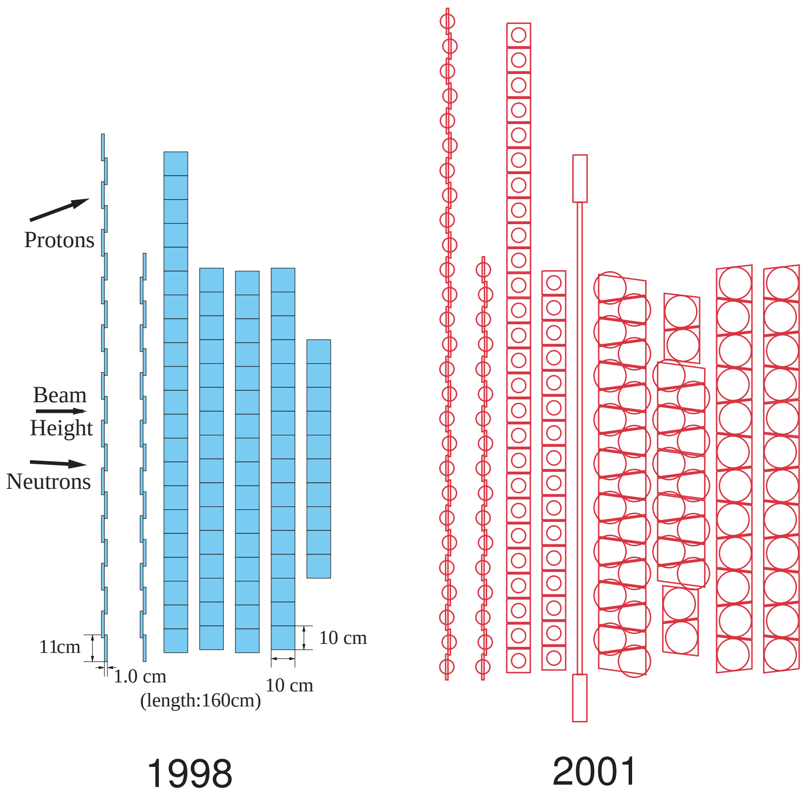

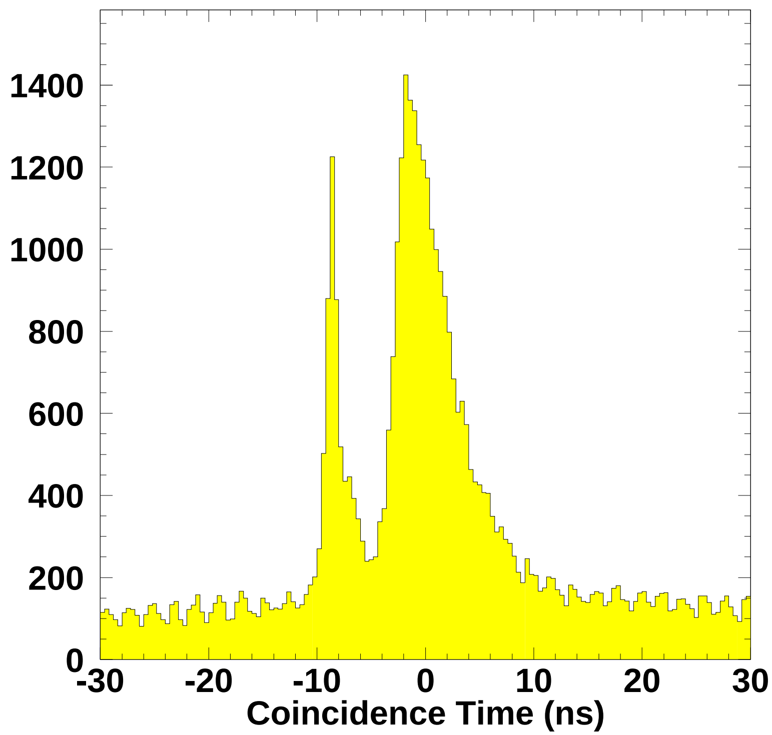

Experimental Technique for $\overrightarrow{\mathrm{D}}(\vec{e}, e'n)p$

For different orientations of h and P: $N^{hP} \propto \sigma(h, P)$

Beam-target Asymmetry:

$$\epsilon = \frac{N^{\uparrow\uparrow} - N^{\downarrow\uparrow} + N^{\downarrow\downarrow} - N^{\uparrow\downarrow}}{N^{\uparrow\uparrow} + N^{\downarrow\uparrow} + N^{\downarrow\downarrow} + N^{\uparrow\uparrow}} = hPfA_{ed}^{V}$$

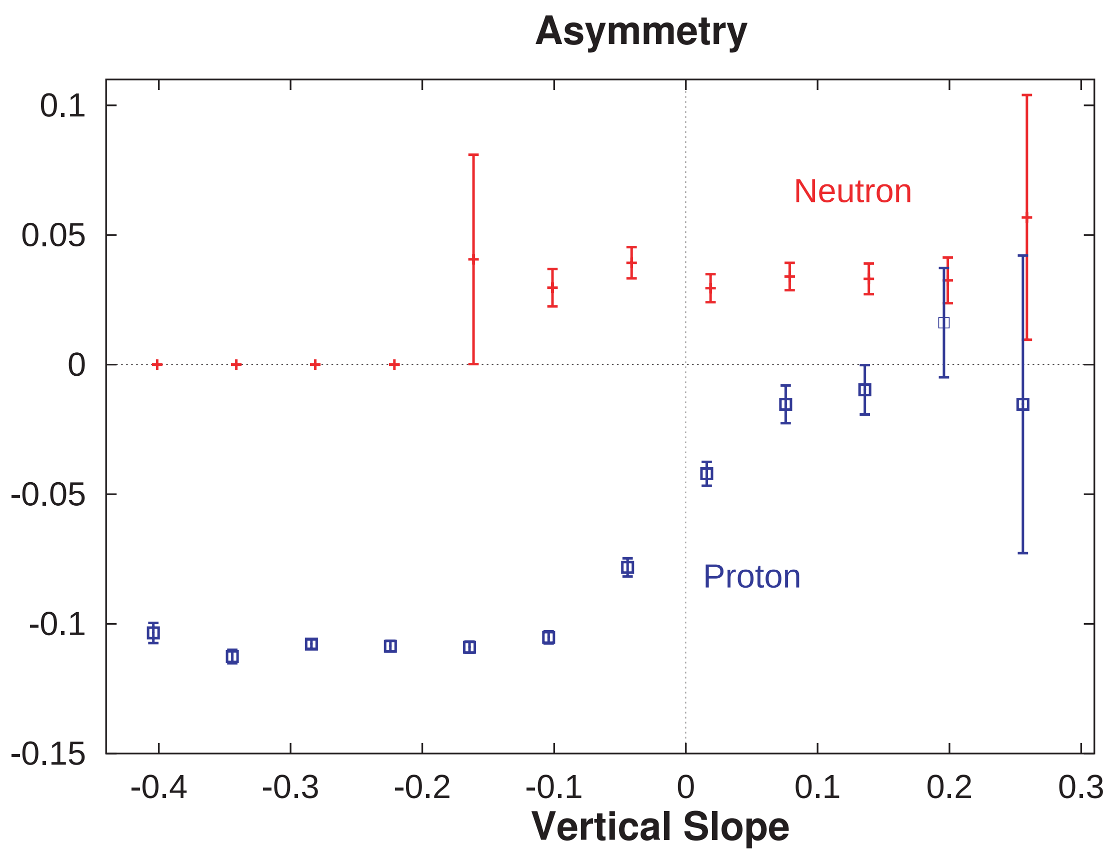

E93026 and World Polarization Data

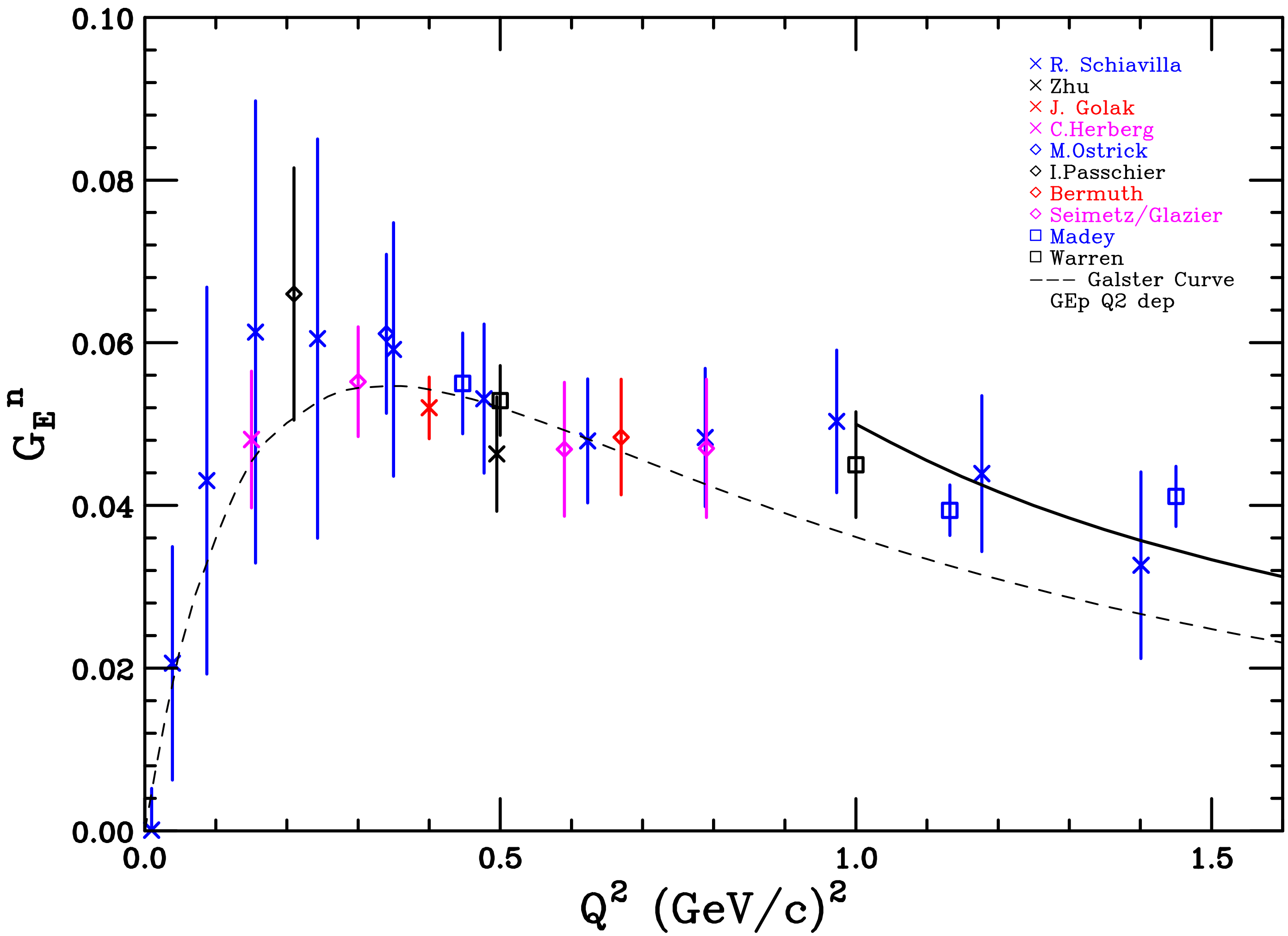

Falls off like proton above $Q^2 = 1$.

Relevant Theories

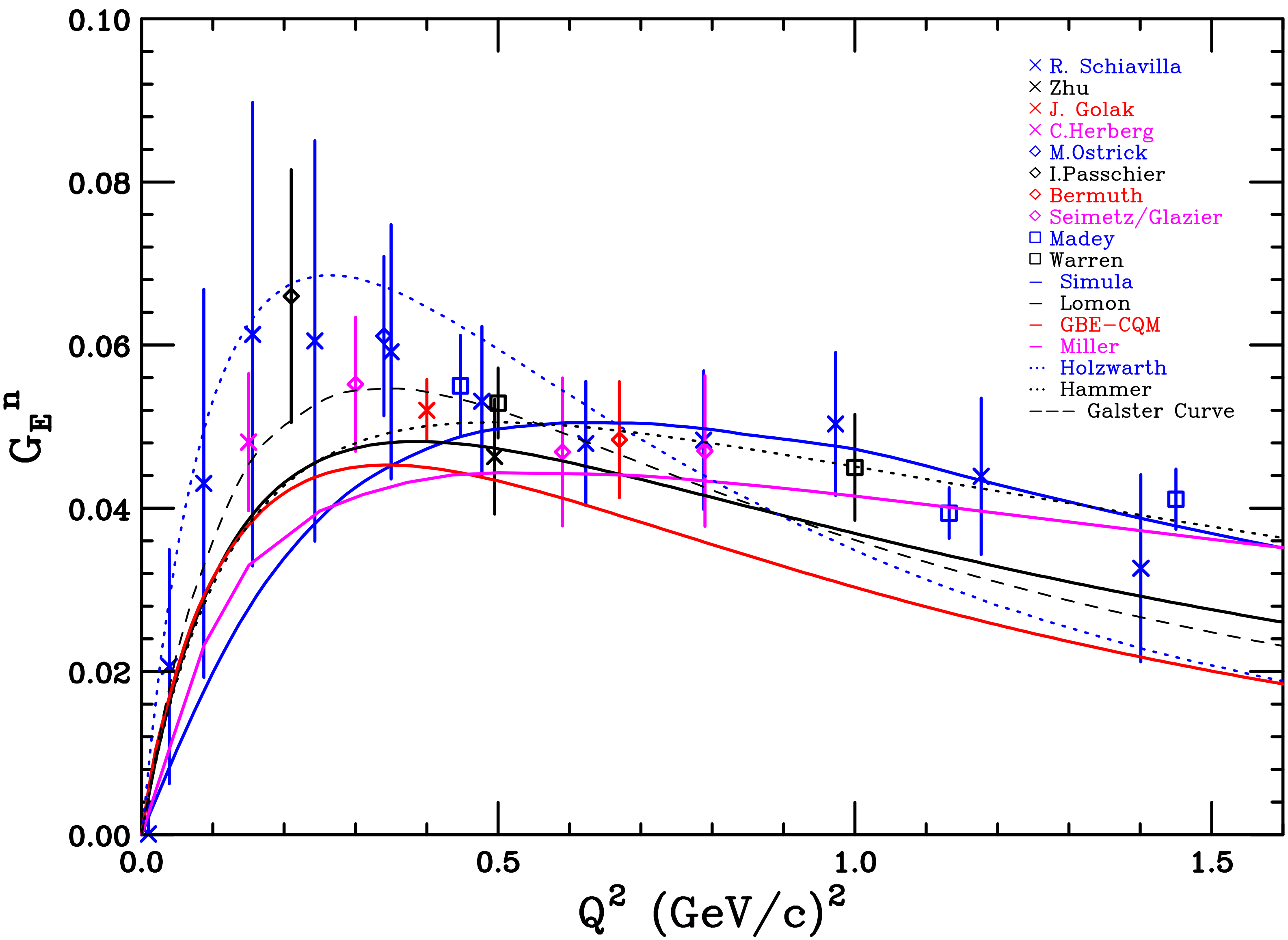

G_M^n via $\overrightarrow{{}^3\mathrm{He}}(\vec{e}, e')X$, E95-001

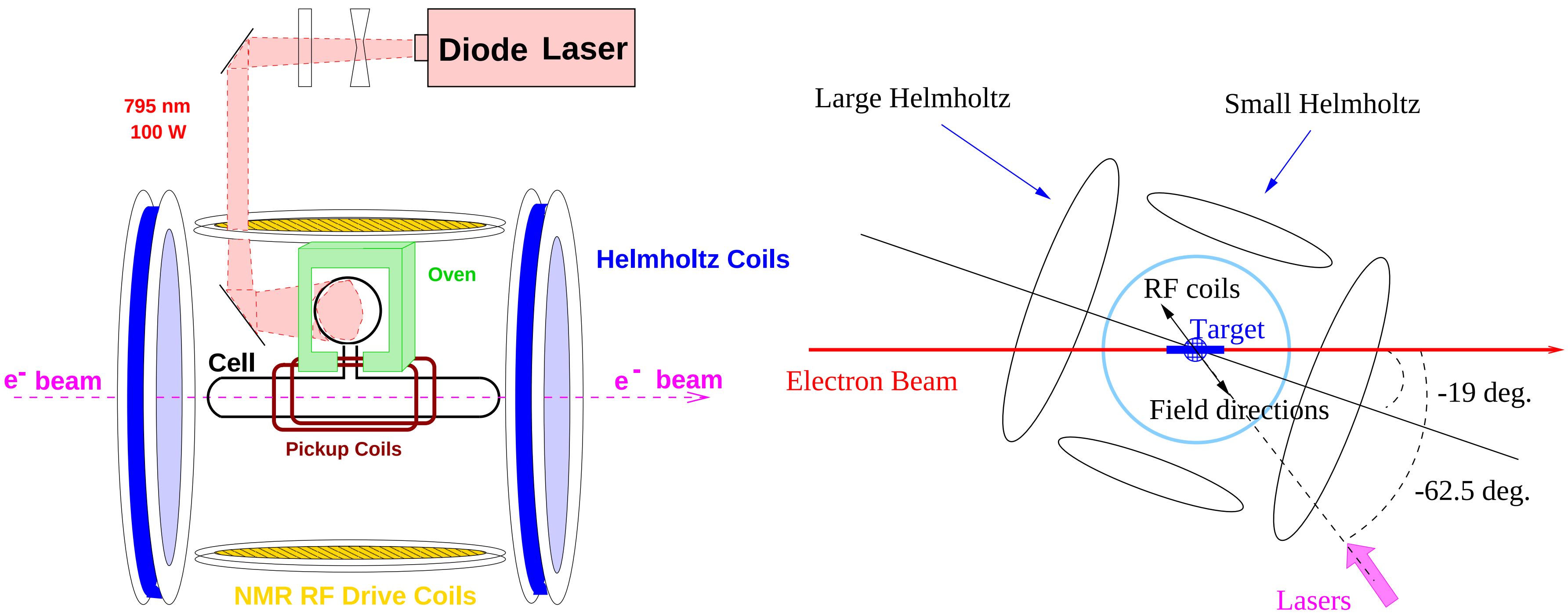

$$A_{\mathrm{raw}}^{\mathrm{qe}} = \frac{Y^{\mathrm{qe}}\uparrow - Y^{\mathrm{qe}}\downarrow}{Y^{\mathrm{qe}}\uparrow + Y^{\mathrm{qe}}\downarrow} = A_{\mathrm{exp}}^{\mathrm{qe}} \times P_b P_t$$

- ✳ Elastic scattering as monitor of $P_b P_t$. Very effective $\rightarrow$ 1.7% contribution to error!
- ✳ P_t^+, P_t^-, h^+, h^- to minimize false asymmetries

G_M^n via $\overrightarrow{{}^3\text{He}}(e,e')X$

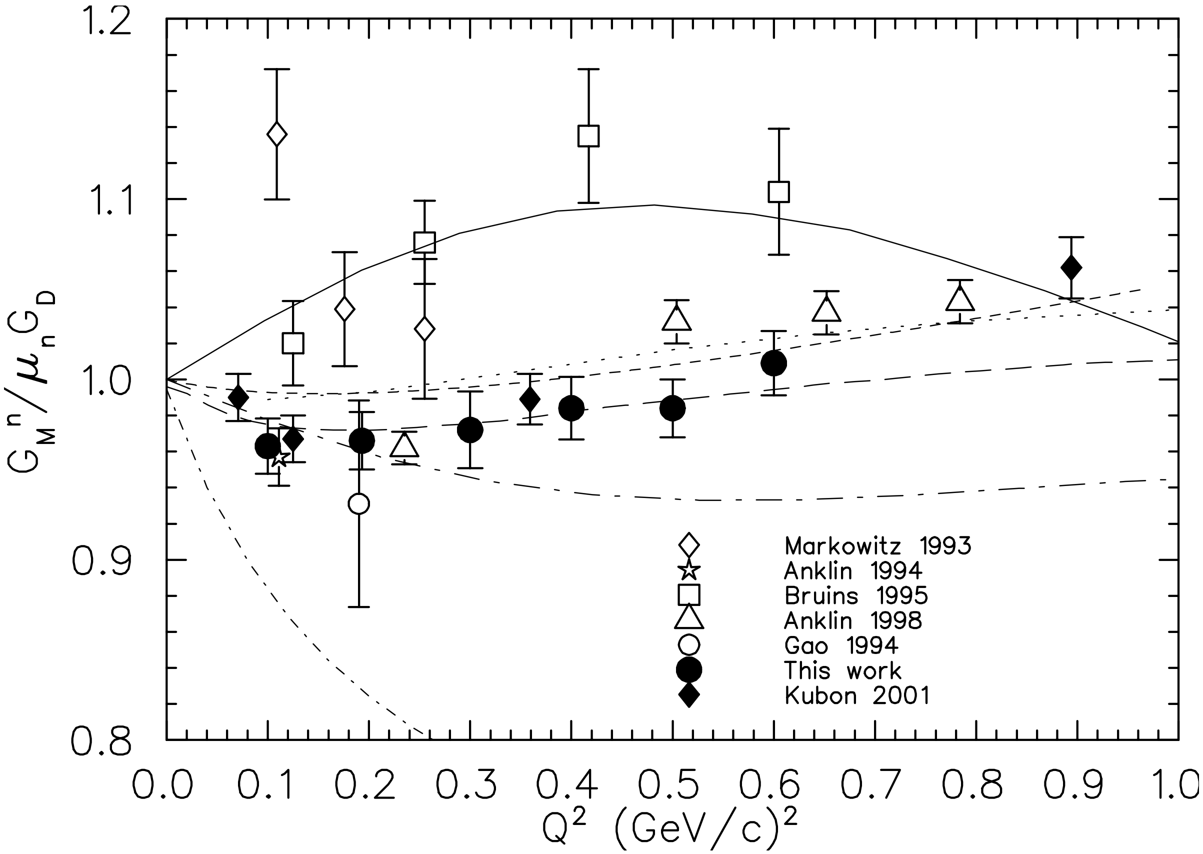

E95001, Wu *et al.*. PRC 67 012201(R) (2003)

- dots: Lomon
- short-dash: Holzwarth
- solid: Lu
- long dash: Mergell

G_M^n at High Q^2 in CLAS

$$R_D = \frac{\frac{d\sigma}{d\Omega}^{D(e,e'n)p}_{QE}}{\frac{d\sigma}{d\Omega}^{D(e,e'p)n}_{QE}} \approx \frac{f(G_M^n, G_E^n)}{f(G_M^p, G_E^p)}$$

Has advantages over $D(e, e')$, $D(e, e'n)p$

- ✴ No Rosenbluth separation or subtraction of dominant proton
- ✴ Ratio insenstive to deuteron model
- ✴ MEC and FSI are small in quasielastic region

✓ Large acceptance to veto events with extra charged particles

✓ Data taken with hydrogen and deuterium target simultaneously

✓ Precise determination of neutron detection efficiency by via $H(e, e'n\pi^+)$

Experimental Advantages/Demands

Using the known values of G_E^p , G_M^p , G_E^n , extract G_M^n .

✳ Insensitive to

- Luminosity
- Electron radiative processes
- Reconstruction and trigger efficiency

✳ Requires

- Precise determination of absolute neutron detection efficiency

Neutron Detection Efficiency

✷ Data taken with hydrogen and deuterium target simultaneously

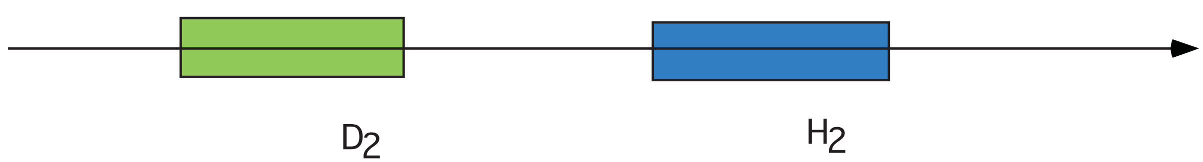

✷ tag neutrons with H_2 target via $H(e, e'n\pi^+)$

– In-situ efficiency, timing, angular resolution determination

– Insensitive to PMT gain variations

– Small acceptance correction

✳ Two beam energies, two field polarities

✳ G_M^n at the same Q^2 in different parts of drift chambers and magnetic field

✳ Neutrons detected in forward calorimeter, large angle calorimeter

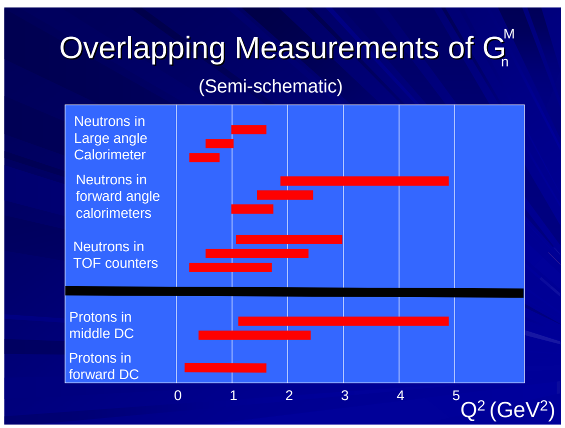

G_M^n Preliminary results from CLAS

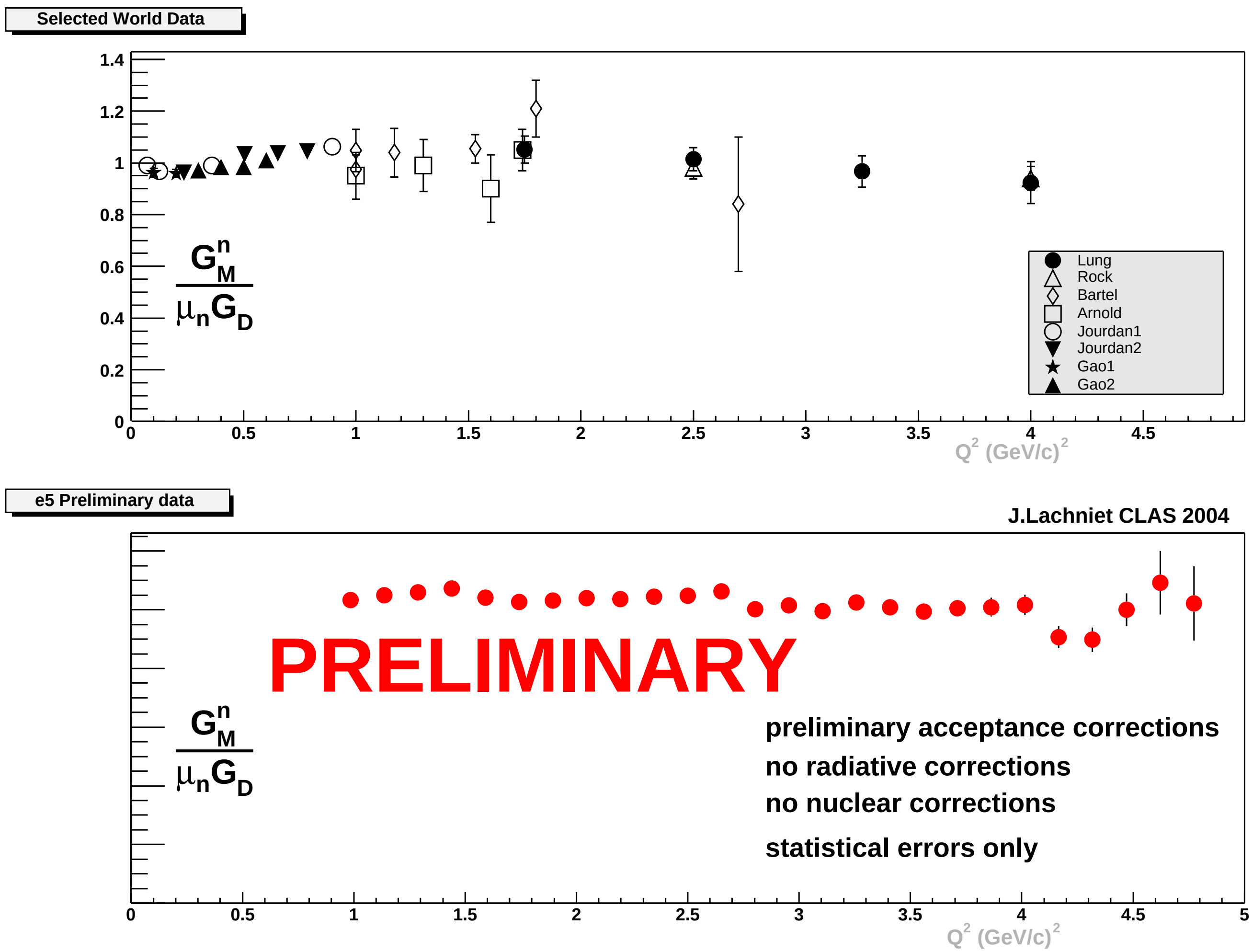

Preliminary results show a minimal deviation from dipole in contrast to the modern parametrization of the historical data set which shows a 10-15% deviation from the new Hall B data.

G_E^p , Status of Rosenbluth Separations

$$\sigma_R \equiv \frac{d\sigma}{d\Omega}\frac{\epsilon(1+\tau)}{\sigma_{Mott}} = \tau G_m^2(Q^2) + \epsilon G_E^2(Q^2)$$

Fundamental problem: σ insensitive to G_E^p at large Q^2. With $\mu G_E^p = G_M^p$, G_E^p contributes 8.3% to total cross section at $Q^2 = 5$.

$$\delta G_E \propto \delta(\sigma_R(\epsilon_1) - \sigma_R(\epsilon_2))(\Delta\epsilon)^{-1}(\tau G_M^2/G_E^2)$$

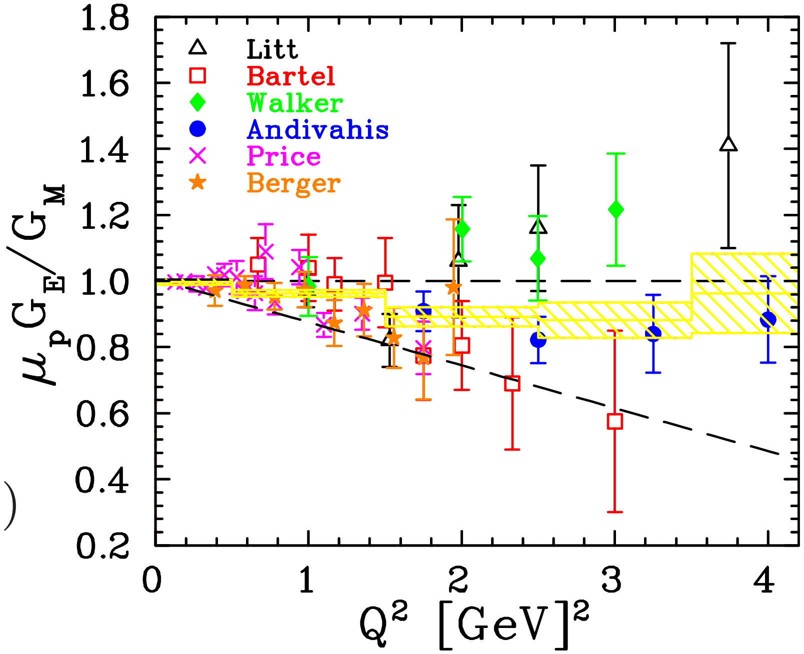

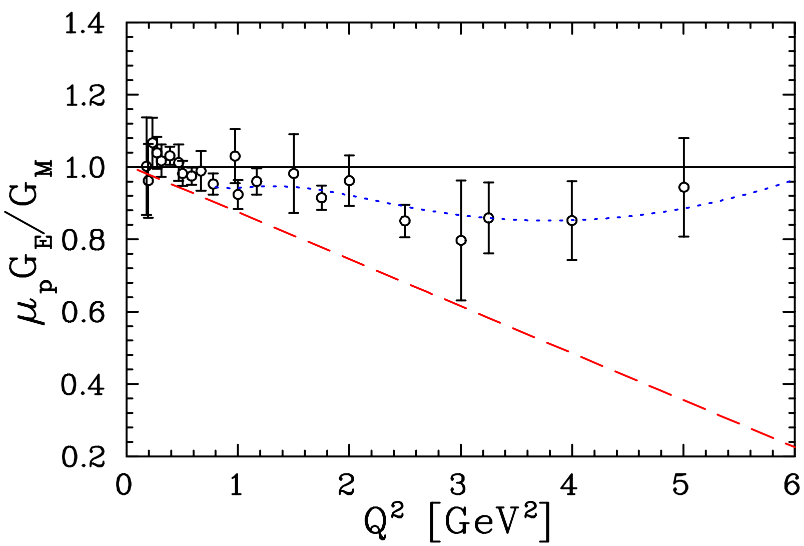

J. Arrington:

Phys. Rev. C68:034325, 2003

- ❑ E94-110 consistent with global fit
- ❑ Rules out experimental systematics
- ❑ ϵ dependence must be large
- ❑ Unconsidered ϵ dependent radiative correction

Super–Rosenbluth, $p(e,p)$

Reduces size of dominant corrections

Rate nearly constant for protons

No p dependent systematics

Sensitivity to angle momentum reduced

Luminosity monitor (second arm)

Background small

Qattan *et al.* nucl-ex/0410010

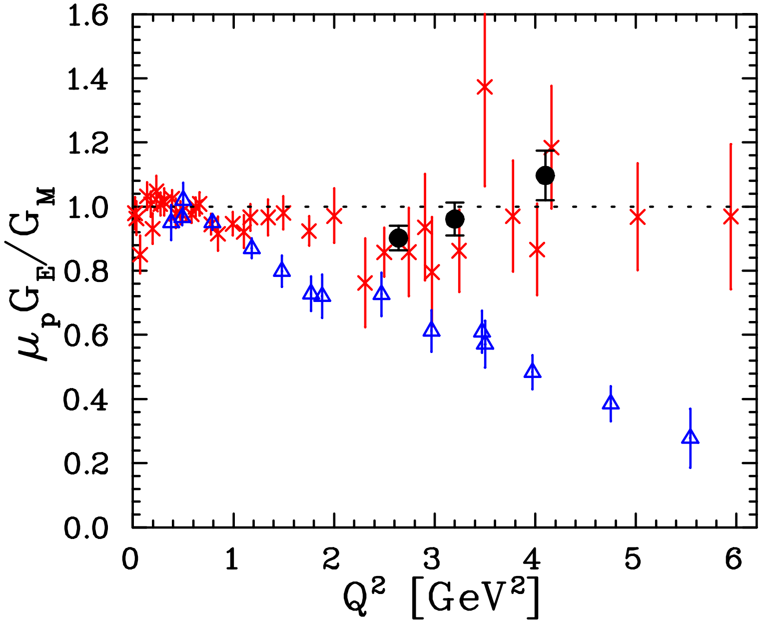

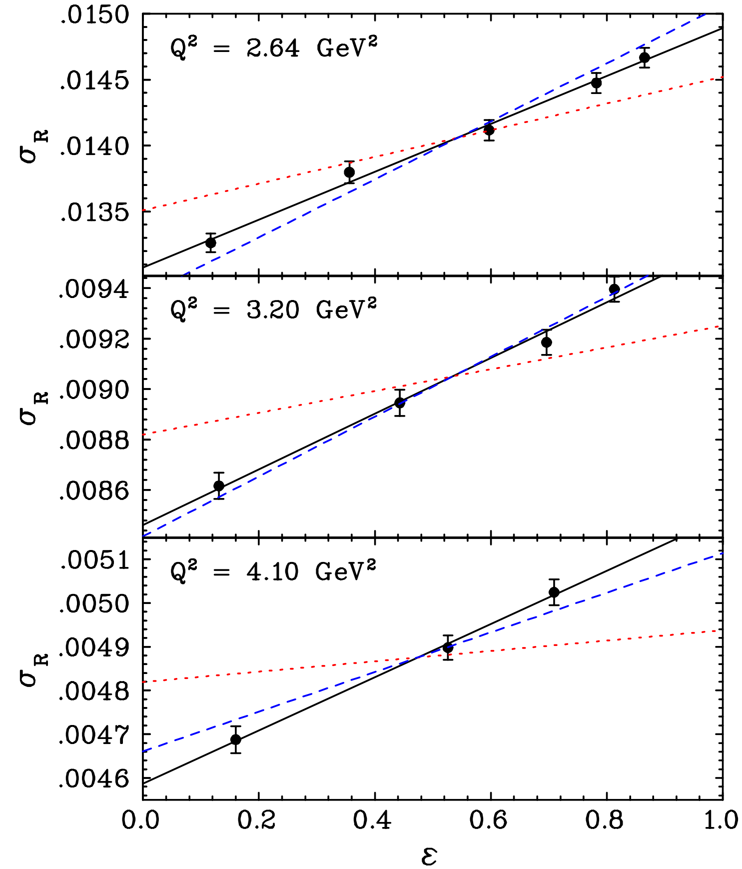

$Q^2 = 3.2$	Electron	Proton
ϵ	0.13–0.87	0.13–0.87
θ	22.2–106.0	12.5–36.3
p [GeV/c]	0.56–3.86	2.47
$\frac{d\sigma}{d\Omega}[10^{-10}]$	6–340	120–170
$\frac{\delta\sigma}{\delta E}[\%/\%]$	11.5–14.2	5.0–5.3
$\frac{\delta\sigma}{\delta\theta}[\%/deg]$	3.6–37.0	5.6–19.0
Rad. Corr.	1.37–1.51	1.24–1.28

Possible explanation: radiative corrections

There are radiative corrections to Rosenbluth experiments that are not included in the analysis

These corrections are: Linear in ϵ and only weakly Q^2 dependent.

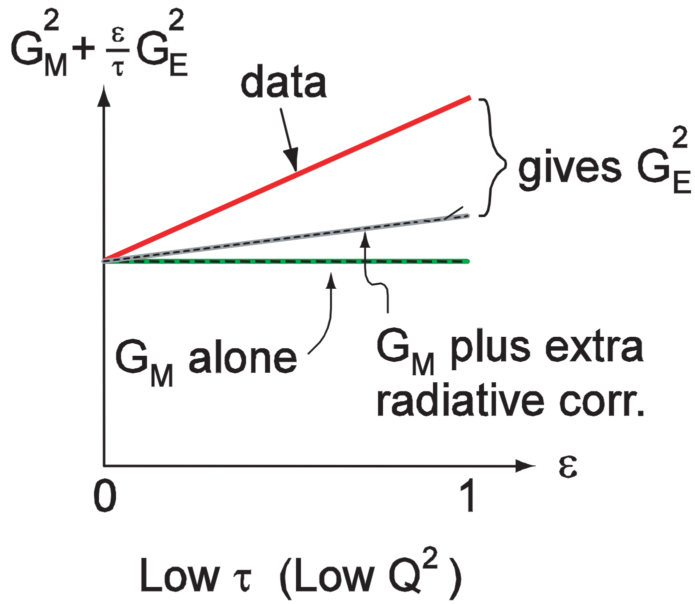

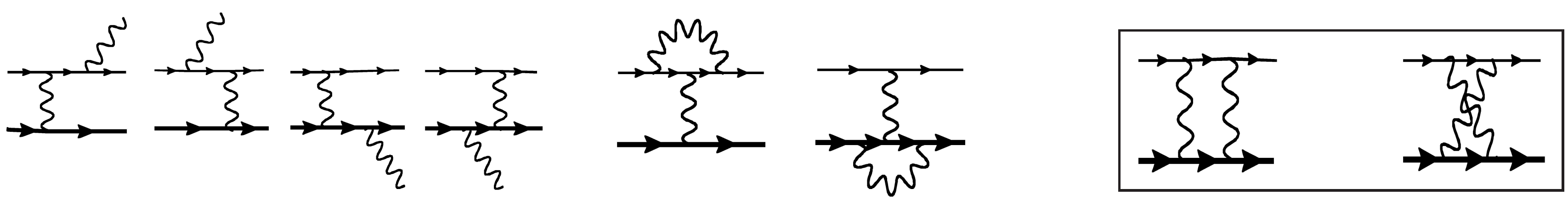

bremsstrahlung

vertex corrections

Two-photon exchange

Two-Photon Contributions

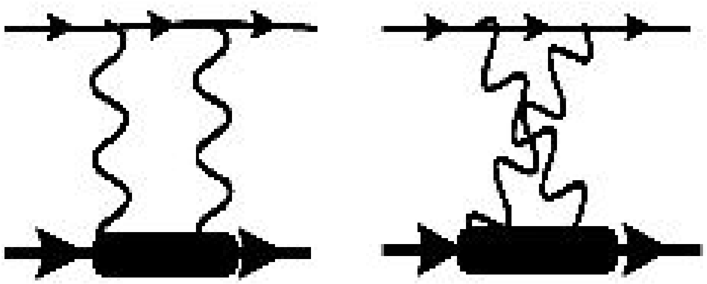

① Rosenbluth formula holds only for single photon exchange

② Certain two-photon processes can occur

③ They are ϵ dependent and can effect the Rosenbluth extraction

④ These have been calculated in the past, but are now being reexamined

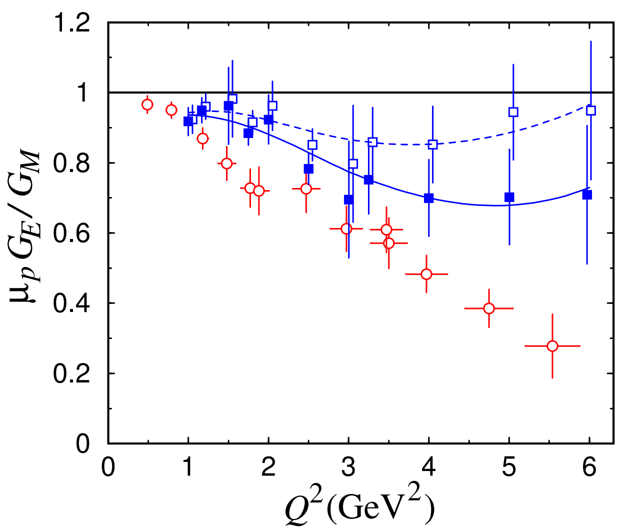

- ✳ In the past, two-photon calculations were done assuming only soft photons so hadronic structure did not play a role
- ✳ Blunden, Melnitchuk and Tjon have done such a calculation: the intermediate state was as nucleon with a monopole form factor.

Two Photon Contributions

Guichon and Vanderhaeghen wrote down general expression and estimated the size of the two-photon contribution required to explaining the discrepancy.

$$\boxed{\frac{d\sigma}{C_B(\varepsilon,Q^2)} \simeq \frac{|\tilde{G}_M|^2}{\tau}\left\{\tau + \varepsilon\frac{|\tilde{G}_E|^2}{|\tilde{G}_M|^2} + 2\varepsilon\left(\tau + \frac{|\tilde{G}_E|}{|\tilde{G}_M|}\right) Y_{2\gamma}(\nu, Q^2)\right\}}$$

$$\boxed{\frac{P_t}{P_l} \simeq -\sqrt{\frac{2\varepsilon}{\tau(1+\varepsilon)}}\left\{\frac{|\tilde{G}_E|}{|\tilde{G}_M|} + \left(1 - \frac{2\varepsilon}{1+\varepsilon}\frac{|\tilde{G}_E|}{|\tilde{G}_M|}\right) Y_{2\gamma}(\nu, Q^2)\right\}}$$

They find $Y_{2\gamma}$ to be on the order of a few % which would generate a 6% correction to the ϵ slope and only slightly modify the recoil polarization results.

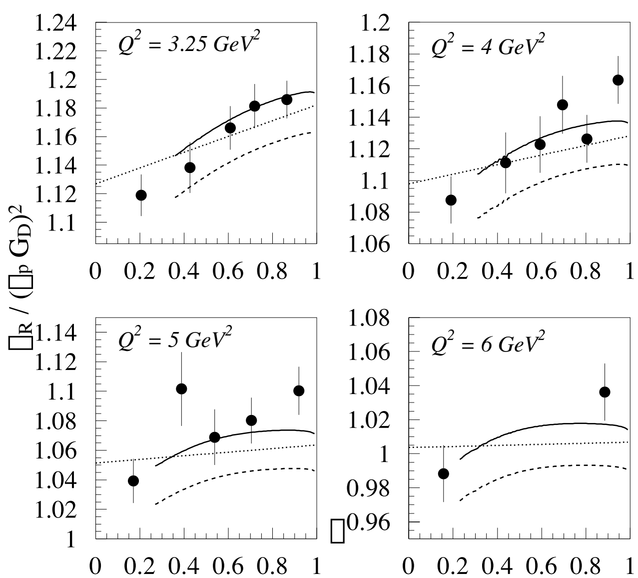

Chen, Afanasev, *et al.* have used a different approach than BMT:

- → hard scattering from quark
- → GPDs describe the quark emission and absorption
- ✔ They argue that when taking the PT form factors as input the addition of the 2–photon correction reproduces the Rosenbluth data

Other work by Tomasi and Rekalo

Two-Photon Contributions

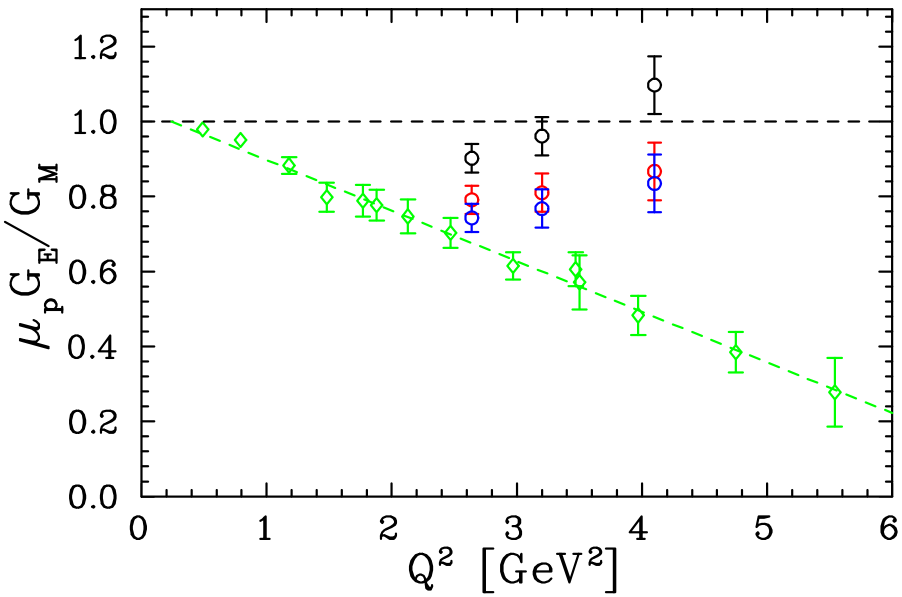

① E01-001 analysis

② TPE of Chen et al.

③ TPE and Coulomb correct. (JA & IS)

④ Still a discrepancy, of which only one-half is explained

J. Arrington, priv. comm.

Experimental Tests are Possible

- ✳ $\frac{\sigma(e^+p)}{\sigma(e^-p)}$
- ✳ Rosenbluth linearity
- ✳ Recoil polarization, p_n
- ✳ $\vec{p}^{\uparrow}(e, e')p$ (SSA)

Notes on two-photon

e^+/e^- and A_y are due to interference of the real parts of the one and two photon terms. Recoil polarization is a measure of the imaginary part

Possible to use elastic electron-nucleon scattering to observe the T-odd parity conserving target single spin asymmetry. It is time reversal odd but A_y does not violate time-reversal invariance.

$A_y = \frac{\sigma_\uparrow - \sigma_\downarrow}{\sigma_\uparrow + \sigma_\downarrow}$

Single spin asymmetry A_y arises from interference between one-photon and two-photon exchange amplitudes and is sensitive to the two-photon exhange amplitude. The normal spin asymmetry is related to the absorptive part of the elastic eN scattering amplitude. Since the one-photon exchange amplitude is purely real, the leading contribution to A_y is of order $O(e^2)$, and is due to an interference between one- and two photon exchange amplitudes.

Data and Theory

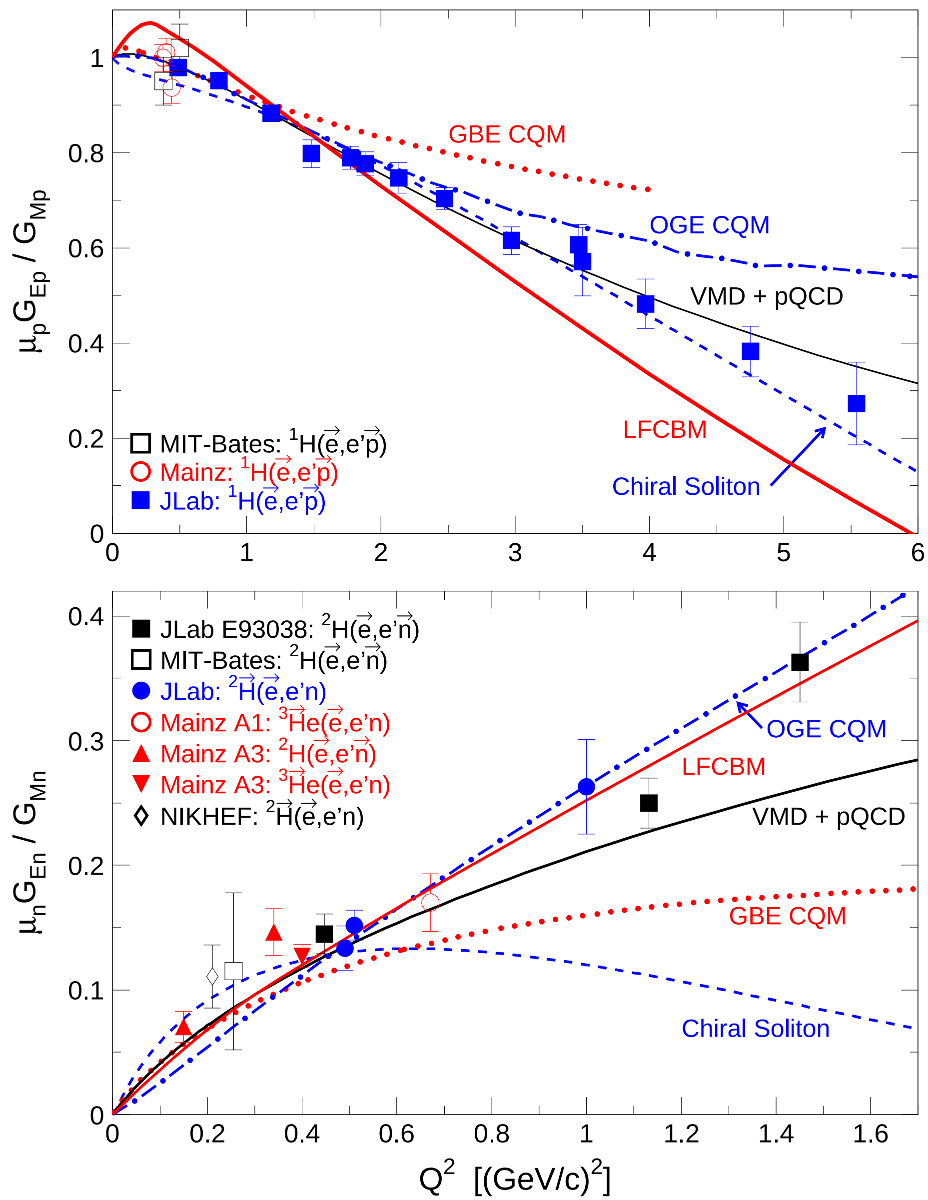

Prospects for future measurements

- Precision measurements of G_E^n out to $Q^2 = 1.5$ (GeV/c)^2 at Mami-C via $^3\overrightarrow{\mathrm{He}}(\vec{e}, e'n)$
- G_E^n via $^3\overrightarrow{\mathrm{He}}(\vec{e}, e'n)$ out to $Q^2 = 3.4$ (GeV/c)^2 in Hall A at JLAB
  - Extension to 5 (GeV/c)^2 in Hall A with 12 GeV upgrade.
- G_E^n via $^2\mathrm{H}(\vec{e}, e'\vec{n})p$ to 4.5 (GeV/c)^2 at JLAB's Hall C
- Precision measurements up to $Q^2 \simeq 1$ (GeV/c)^2 of G_E^n and G_E^p with internal polarized targets and BLAST.
- Form factor ratio (G_E^p/G_M^p) out to 9 (GeV/c)^2 via $^1\mathrm{H}(\vec{e}, e'\vec{p})$ in Hall C at JLAB with 6 GeV beam, 2005-2006.
  - Extension out to 12.4 (GeV/c)^2 with 12 GeV upgrade.
- G_M^n out to 14 (GeV/c)^2 with an upgraded CLAS and 12 GeV upgrade.
- G_M^p to 8 (GeV/c)^2 (as part of new proposal to measure $B(Q^2)$ at 180 degrees in Hall A).

Conclusion

- Outstanding data on G_E^p out to high momentum transfer – spawning a tremendous interest in the subject and the re-evaluation of our long held conception of the proton.
- Finally G_E^n measurements of very high quality from Mainz and Jefferson Lab out to 1.5 (GeV/c)^2 exists, allowing rigorous tests of theory.
- Data sets out to large Q^2 from future experiments will further constrain any model which attempts to describe the nucleon form factors.
- A resolution of the G_E^p data from recoil polarization and Rosenbluth techniques will have applications in similar experiments from nuclei and deepen our understanding of physics and experiment.

Although the major landmarks of this field of study are now clear, we are left with the feeling that much is yet to be learned about the nucleon by refining and extending both measurement and theory. *R.R. Wilson and J.S. Levinger, Annual Review of Nuclear Science, Vol. 14, 135 (1964).*